NTNU – Trondheim
Norwegian University of
Science and Technology

Correlation between SPT and CPT

Odong Guen

Geotechnics and Geohazards
Submission date: June 2014
Supervisor: Gudmund Reidar Eiksund, BAT

Norwegian University of Science and Technology
Department of Civil and Transport Engineering

NORWEGIAN UNIVERSITY OF SCIENCE AND TECHNOLOGY
DEPARTMENT OF CIVIL AND TRANSPORT ENGINEERING

Report Title: SPT-CPT correlation	Date: June 10th 2014 Number of pages (incl. appendices): 99			
	Master Thesis	v	Project Work	
Name: Guen, Odong				
Professor in charge/supervisor: Gudmund Reidar Eiksund				
Other external professional contacts/supervisors:				

Abstract:
The objectives of this thesis are to introduce and describe SPT, CPT methods and the correlation between them. Moreover, it is explained how the correlation between SPT and CPT is reliable and what kinds of studies are needed to improve the reliability of the correlation between q_c/N and D_{50}.

Standard Penetration Test (SPT) is internationally used in-situ test to investigate soil properties under the ground. However, it has problems regarding the repeatability and reliability even if geotechnical engineers have tried to standardize the SPT procedure. The Cone Penetration Test is becoming significantly popular in-situ test to investigate a site and to do geotechnical design. It is useful in-situ test to delineate stratigraphy and to continuously measure parameters such as q_c and f_s. The merits of CPT method as the soil investigation tool are the repeatability, continuous record and simplicity.

A large amount of data has been built based on the SPT so that it is needed to use the data with the introduction of the CPT method. First chapter is a short introduction about SPT and CPT methods. Chapter 2 shows how the SPT was made and how the energy is travelled in the rod when the hammer hit it. In addition, what kinds of factors affect the N-value, how other parameters are related to the N-value and how SPT is applied are shown. Chapter 3 introduces the four cone penetration tests types, how CPT is applied and what kinds of parameters can be estimated from the CPT. In Chapter 4 I have illustrated some examples where the correlation between SPT and CPT was studied. In these various soils the correlation between q_c/N and D_{50} is useful, but in other cases it may be not reliable. Therefore, more samples are needed to sharpen the reliability of the correlation between q_c/N and D_{50} and other studies are recommended to improve the reliability of the correlation between q_c/N and D_{50}.

Keywords:

1. SPT
2. CPT
3. SPT-CPT correlation
4. q_c/N

Odong G.

NTNU
Faculty of Engineering Science and Technology
Institute of Civil and Transport Engineering

MASTER DEGREE THESIS

Spring 2014
for

Student: **Odong Guen**

Correlations between the Standard Penetration Test and the Cone penetration test

BACKGROUND

The Standard Penetration Test (SPT) has been used extensively used for many decades. The Cone Penetration Test (CPT) is however becoming increasingly more popular. Utilization of the large test database from SPT in combination with CPT tests measurements will be valuable for engineering practice. To achieve this, correlations between soil parameters derived from Standard Penetration Test and Cone penetration test are needed.

TASK

Task description

The thesis should include a description the methods and a literature study on correlations between the SPT and CPT. The thesis should also address factors that affect the reliability of the correlations between the methods. Examples may be the effect of rod length, effect of borehole diameter and rod energy ratio. It is of interest to see how CPT and SPT results may be applied for liquefaction assessment and design of pile foundations.

Objective and purpose

The work aims at describing the correlation between CPT and SPT.

Subtasks and research questions

- Description of the soil SPT and the CPT test methods
- Literature review on SPT – CPT correlations
- Evaluation of the soil parameters usually derived from the methods and evaluation of the reliability

General about content, work and presentation

The text for the master thesis is meant as a framework for the work of the candidate. Adjustments might be done as the work progresses. Tentative changes must be done in cooperation and agreement with the professor in charge at the Department.

In the evaluation thoroughness in the work will be emphasized, as will be documentation of independence in assessments and conclusions. Furthermore the presentation (report) should be well organized and edited; providing clear, precise and orderly descriptions without being unnecessary voluminous.

The report shall include:

- Standard report front page (from DAIM, http://daim.idi.ntnu.no/)
- Title page with abstract and keywords.(template on: http://www.ntnu.no/bat/skjemabank)
- Preface
- Summary and acknowledgement. The summary shall include the objectives of the work, explain how the work has been conducted, present the main results achieved and give the main conclusions of the work.
- The main text.
- Text of the Thesis (these pages) signed by professor in charge as Attachment 1.

The thesis can as an alternative be made as a scientific article for international publication, when this is agreed uponbythe Professor in charge. Such a report will include the same points as given above, but where the main text includes both the scientific article and a process report.

Advice and guidelines for writing of the report is given in "Writing Reports" by Øivind Arntsen,and in the departments "Råd og retningslinjer for rapportskriving vedprosjekt og masteroppgave"(In Norwegian)located at http://www.ntnu.no/bat/studier/oppgaver.

Submission procedure

Proceduresrelating to the submissionof the thesis aredescribedin DAIM (http://daim.idi.ntnu.no/). Printing ofthe thesis isordered through DAIMdirectly toSkipnesPrintingdeliveringthe printedpaperto the departmentoffice2-4 dayslater.The departmentwill payfor 3copies, of whichthe instituteretainstwocopies.Additional copiesmust bepaid for by thecandidate/ externalpartner.

On submissionof the thesisthe candidate shallsubmit aCD withthe paperin digitalform inpdf andWordversion, the underlyingmaterial (such asdata collection)in digitalform (e.g. Excel). Students mustsubmitthe submissionform(fromDAIM) where both theArk-BiblinSBIand PublicServices(Building Safety) of SBII hassignedthe form.The submission form includingthe appropriatesignatures must be signed bythe departmentofficebefore the formis deliveredFacultyOffice.

Documentation collected during the work, with support from the Department, shall be handed in to the Department together with the report.

According to the current laws and regulations at NTNU, the report is the property of NTNU. The report and associated results can only be used following approval from NTNU (and external cooperation partner if applicable). The Department has the right to make use of the results from the work as if conducted by a Department employee, as long as other arrangements are not agreed upon beforehand.

Tentative agreement on external supervision, work outside NTNU, economic support etc.
Separate description is to be developed, if and when applicable. See http://www.ntnu.no/bat/skjemabank for agreement forms.

Health, environment and safety (HSE)http://www.ntnu.edu/hse
NTNU emphasizes the safety for the individual employee and student. The individual safety shall be in the forefront and no one shall take unnecessary chances in carrying out the work. In particular, if the student is to participate in field work, visits, field courses, excursions etc. during the Master Thesis work, he/she shall make himself/herself familiar with "Fieldwork HSE Guidelines". The document is found on the NTNU HMS-pages at http://www.ntnu.no/hms/retningslinjer/HMSR07E.pdf

The students do not have a full insurance coverage as a student at NTNU. If you as a student want the same insurance coverage as the employees at the university, you must take out individual travel and personal injury insurance.

Startup and submission deadlines
Startup for this thesis is January 15th 2014. The thesis should be submitted electronically in DAIM before June 11th 2014.

Professor in charge: Gudmund Eiksund

Department of Civil and Transport Engineering, NTNU
Date: 15.01.2014, (revised: 06.06.2014)

Gudmund Eiksund

Professor in charge (signature)

Acknowledgements

This thesis was performed as a part of the Geotechnics and Geohazards International Master Program at the Norwegian University of Science and Technogoloy (NTNU). How SPT and CPT work and how they are applied is explained. The studies of the correlation between SPT and CPT are explained.

I would like to show my gratitude to all those who have helped and continue to help me. I want to thank to the professor, Gudmund Eiksund, who is also my thesis supervisor, thank to my family, Young Uoon Guen, Jin Suk Lee and Oh Tae Kwon, who support me from Korea and last but not least I would like to thank to Dong-hoi Kim who studies in NTNU and helps me a lot.

Trondheim, June 10th 2014

Guen, Odong

Table of Contents

List of Figures

List of Table

Notations

English

A	Cross-sectional area
B	Width of foundation
Bq	Normalized pore pressure ratio
B_q	Pore pressure ratio
b	Pile diameter
C_B	Borehole diameter correction
C_E	Correction for rod energy
C_K	A coefficient
C_N	Correction by effective overburden stress
C_Q	Normalization factor for cone penetration resistance
C_R	Rod length correction
C_{OCR}	A coefficient
C_S	Shaft correlation coefficient(in pile design)
C_S	Correction by the sampling method
C_t	Toe correlation coefficient
C_u	Undrained shear strength
C_φ	A coefficient
c	Speed of the stress wave spread
D_r	Relative density
D_{50}	Mean grain size
d	Diameter of pile
E	Elasticity modulus of the drill rod
E_m	Hammer efficiency
E_u	Undrained Young´s modulus
E´	Drained Young's modulus
F	Gauged force the around the peak of the drill rod depending on time
F_i	Force in the incident wave
F_r	Normalized friction ratio in CPT_u
F_r	Force in the reflected wave
F_t	Force in the transmitted wave
f_b	Toe resistance
f_s	Cone sleeve friction
f_s	Shaft resistance in pile design
f_2	Coefficient
G	Shear modulus
G_O	Strain stiffness

H_e	Embedment depth of foundation
I_c	Soil behavior type index
K	Coefficient in end bearing resistance
K_O	In-situ stress ratio in overconsolidated sand
K_O	Earth stress coefficient
K_{ONC}	In-situ stress ratio in normally consolidated sand
K_φ	A coefficient
k	Hydraulic conductivity
L	Length of pile
M	Constrained modulus
M_w	Moment magnitude of earthquake
m_v	Coefficient of volume compressibility
N	Raw blow count
N_{kt}	A coefficient
N_1	Corrected N value by 100 kPa effective overburden pressure
$(N_1)_{60}$	Corrected N value by vertical effective stress and input energy
$(N_1)_{60cs}$	$(N_1)_{60}$ adjusted to equivalent clean-sand value
N_{60}	Corrected N value by 60 percent of theoretical free-fall hammer energy
N´	Corrected N value by 100 kPa effective overburden pressure
$\overline{N}$	Average N-value
n	Exponent employed in normalizing CPT resistance for overburden stress
P_a	Atmospheric pressure 100kPa
P_L	Probability of liquefaction
Q_t	Normalized cone resistance
q_c	Cone penetration resistance
q_{c1N}	Normalized cone penetration resistance
$(q_{c1N})_{cs}$	Normalized cone penetration resistance adjusted to equivalent clean-sand value
q_E	Cone stress after correction for pore pressure
q_{Eg}	Geometric average of the cone stress over the influence zone
q_t	Cone resistance corrected by pore water pressure
q_{ult}	Ultimate bearing stress for foundation system
R_f	Normalized friction ratio
R_k	Bearing factor term for foundations on clay
r_s	Pile unit shaft resistance
r_t	Pile unit toe resistance
S_u	Undrained shear strength
S_t	Sensitivity
t´	Time when the initial force measurement moves through zero
u_o	Hydraulic pore pressure
u_2	Pore pressure measured with a porous filter

V_s	Shear wave velocity
v	Velocity gauged depending on time
v	Impact velocity
v_h	Particle velocity in the hammer
v_i	Velocity in the incident wave
v_r	Particle velocity in the rod
v_t	Velocity in the transmitted wave
w	Water content
z_e	Foundation embedment depth

Greek

α	Material ratio
α	A coefficient (1.5 to 4) changed depending on the cohesive soil types and cone resistance in constrained modulus
α	A_n/A_c
α	Coefficient that are functions of fines content, used to correct $(N_1)_{60}$ to $(N_1)_{60cs}$
α	Parameter gained through empirical correlations
β	Parameter gained through empirical correlations
β	Coefficient that are functions of fines content, used to correct $(N_1)_{60}$ to $(N_1)_{60cs}$
γ	Unit weight
γ_w	Unit weight of water
σ_{atm}	Atmospheric pressure
σ_h'	Horizontal effective stress
σ_{vo}	Total vertical(overburden) stress
σ_{vo}'	Vertical effective stress
σ_z'	Vertical effective stress
τ_u	Undrained shear strength
φ'	Friction angle
ΔU	u_2-u_o

Abbreviation

BC	Bearing Capacity
CPT	Cone Penetration Test
CPT_u	Cone Penetration Test with Pore Pressure
CRR	Cyclic Resistance Ratio
$CRR_{7.5}$	Cyclic Resistance Ratio for M_w=7.5 Earthquakes
CSR	Cyclic Stress Ratio
FC	Fines Content
LCPC	Laboratoire Central des Ponts et Chausees

NCEER	National Center for Earthquake Engineering Research
OCR	Overconsolidation Ratio
SBT	Soil Behavior Type
SCPT	Seismic Cone Penetration Test
SPT	Standard Penetration Test

Summary

The objectives of this thesis are to introduce and describe SPT, CPT methods and the correlation between SPT and CPT. Moreover, it is explained how the correlation between SPT and CPT is reliable and what kinds of studies are needed to improve the reliability of the correlation between q_c/N and $D_{50,}$

Standard Penetration Test (SPT) is internationally used in-situ test to investigate soil properties under the ground. However, it has problems regarding the repeatability and reliability even if geotechnical engineers have tried to standardize the SPT procedure. The Cone Penetration Test is becoming significantly popular in-situ test to investigate a site and to do geotechnical design. It is useful in-situ test to delineate stratigraphy and to continuously measure parameters such as q_c and f_s. The merits of CPT method as the soil investigation tool are the repeatability, continuous record and simplicity.

A large amount of data has been built based on the SPT so that it is needed to use the data with the introduction of the CPT method. First chapter is a short introduction about SPT and CPT methods. Chapter 2 shows how the SPT was made and how the energy is travelled in the rod when the hammer hit it. In addition, what kinds of factors affect the N-value, how other parameters are related to the N-value and how SPT is applied are shown. Chapter 3 introduces the four cone penetration tests types, how CPT is applied and what kinds of parameters can be estimated from the CPT. In Chapter 4 I have illustrated some examples where the correlation between SPT and CPT was studied. It is showed that in these various soils the correlation between q_c/N and D_{50} is generally reliable.

1 Introduction

1.1 Introduction

The Standard Penetration Test (SPT) is the most normally employed in-situ test even though it has problems with the repeatability and reliability. SPT does not mean that it is "standard" as the name indicates. Even though the test is simple to use, it can yield N-value and a soil sample for laboratory test so that it is widely used by geotechnical engineers. N-value helps to produce many correlations with parameters such as pile side friction, allowable bearing capacity, relative density and friction angle. SPT are widely used to know the soil parameters by using the correlations (Davidson, Maultsby, & Spoor, 1999).

The Cone Penetration Test (CPT) is becoming significantly popular in-situ test to do site investigation and do geotechnical design. It is useful for stratigraphy delineation and continuous fast record of parameters such as cone tip resistance (q_c) and sleeve friction (f_s). The merits of the CPT are the repeatability, continuous measurement, and simplicity(P. Robertson, Campanella, & Wightman, 1983).

The Standard Penetration Test (SPT) is widely employed in-situ test. Even though there have been continuous attempts to standardize the

SPT process, it is still hard problems for geotechnical engineers to have the reliability and repeatability of the SPT. A significant experience related to the design methods from the local SPT correlation has been built. However, with time passed, direct CPT design interactions will be grown as well on the basis of local experience and field examination. Therefore, it is necessary to make correlation between SPT and CPT in order to use SPT-based data that already exist(P. Robertson et al., 1983).

1.2 Objectives

The correlation between SPT and CPT was introduced to use many SPT-based data. The objectives of this thesis are to introduce SPT, CPT and the correlation between SPT and CPT. It is also explained how the correlation between q_c/N and D_{50} is reliable and what kinds of studies are needed to sharpen the reliability of the correlation between q_c/N and D_{50}. First chapter is a short introduction about SPT and CPT methods. Chapter 2 shows how the SPT was made and how the energy is travelled in the rod when the hammer hit it. In addition, what kinds of factors affect the N-value, how other parameters are related to the N-value and how SPT is applied are shown. Chapter 3 introduces the four cone penetration tests types. How CPT is applied and what kinds of parameters can be estimated from the CPT is shown. In Chapter 4 I have illustrated some examples where the correlation between q_c/N and D_{50} was studied. Chapter 5 explains how the correlation between q_c/N and D_{50} is reliable in various soils. Chapter 6 shows what kinds studies are needed to improve the reliability of the correlation between q_c/N and D_{50}.

2 Standard Penetration Test

2.1 Standard penetration test

The Standard Penetration Test, SPT was developed in America in 1927 and is still internationally used in-situ test to investigate soil properties under the surface. The test has evolved from a personally devised and provincially used test into a widely used test for soil investigation. The test is made up of dropping a 140 lb (63.5kg) hammer for a free falling of 12 inches (30cm) to give impact to the top of a rod to which a split-spoon sampler is attached to the lower end. Figure 2.1 shows the usual split-spoon sampler and the types of samplers are shown in Table A-1. The blow number to drive the sampler 12 inches (30cm) into the ground is called the SPT N value or blow count. The normal process is to push the rod into the end of a borehole and to store information about the number of blows each 6 inch (15cm) interval for the first 18 inches (45cm) of driving (Aboumatar, 1994).

2.1.1 Advantages of the Standard Penetration Test

There are significant advantages of the SPT tests. The equipment is relatively rugged and simple, it is easy to handle the procedures and do frequent tests, soil sample is commonly gained, this tests can be treated

in many soils, useful correlations have been found through this test and this test has very flexibility (P. K. Robertson, Woeller, & Addo, 1992).

2.1.2 Disadvantages of the Standard Penetration Test

The SPT procedure has reliability when the soil type is the granular soils like sand and granule gravel. The SPT shows the different driving resistances in the silts and clays when they are dry or moist. When the sampler faces rocks larger than the sample barrel's sleeve diameter, interpretive problems can happen in the SPT procedure. In these situations, high blow numbers can be recorded and theses horizons can be considered wrongly as "bedrock" or "drilling refusal" with ease as shown in Figure 2.3(Rogers, 2006).

The influence of the strata thickness and stiffness's change is also the problem as represented in Figure 2.4. When the sample barrel comes near a significantly stiffer horizon, although the material which are sampled remains consistent around the softer horizon the penetration resistance will improve. This can overestimate strength, density, and compressibility. In addition, a big disadvantage of SPT process that it informs the average blows per foot during sample round and the measurement would be particularly accurate for horizons larger than 12 in (30.5cm) thick as well as for the influence area beneath the sampler shoe showed in Figure 2.4 (Rogers, 2006).

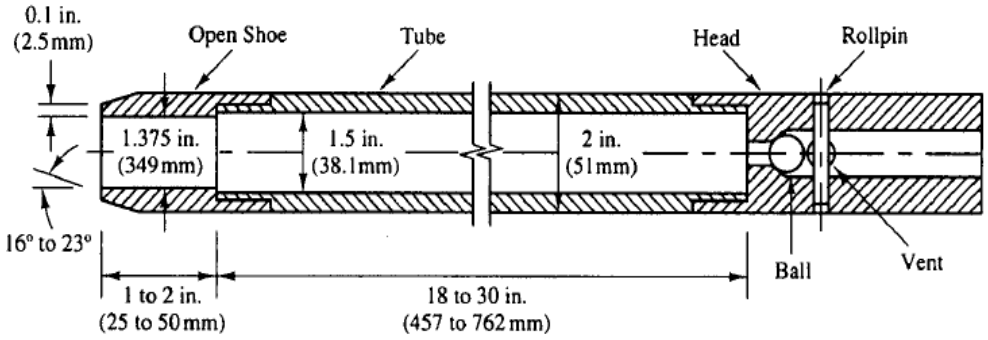

Figure 2.1 A Normal Split Spoon Sampler (ASTM, 1984)

2.2 History of the Standard Penetration Test

The Standard Penetration Test appeared as outcomes of the evolution of dry sample recovery skills. Formerly only through the use of wash bor-

ings, investigations under the ground were generally achieved. A wash boring connect with the circulation of a water and/or drilling mud blend to get rid of the cuttings from the boring as the hole is developed. The first technique of dry sample recovery was suggested by Charles R. Gow in 1902. He utilized a 110 lb (50kg) weight to push a one inch outside width sampling pipe. After this technique was employed for a short time, it came clear that the condition and characteristic (e.g., strength and density) of the soil affected the resistance to pushing the sampler. Therefore, "penetration resistance" was employed to represent the number of blows to drive the sampler a given length (Aboumatar, 1994).

In 1922, the Charles R. Gow Company incorporated with the Raymond Concrete Pile Company where L. Hart and G.A. Fletcher came up with a split-spoon sampler (1927) of 2 inches width which is very analogous to the present Standard Penetration Test shown in Figure 2.1. The first steps were initiated through the attempts of Gordon Fletcher, Linton Hart and Harry Mohr in the end 1920's. The drive height was placed at 30 inches (76cm) and the drive weight was altered from 110lb (50kg) to 140lb (63.5kg). After wide-ranging field and laboratory performance, blow count to drive the sampler into the soil a length of 12 inches (30cm) was found as an authorized record of the test(Aboumatar, 1994).

The test stayed fundamentally without any changes until 1954 when James Parsons suggested a mean of storing information about the blow count after the primary work in the later 1920's. In place of a thrust of 12 inches (30cm) the sampler was pushed into the soil and the blow count was recorded for each increase of 6 inches (15cm). Then the two smallest 6 inch (15cm) increased blow counts were counted up and registered as the blow count. Since 1954, the mean of storing information about the blow count has been changed in the test but the sampler is still driven 18 inches (45cm) into the soil. The required blow count to penetrate first 6 inches (15cm) is registered but the blow count is regarded as a seating drive. Even though blow count for 6 inch (15cm) increase is usually registered, the blows are the recorded blow count (N value) when the sampler drive the last 12 inches (30cm) (Aboumatar, 1994).

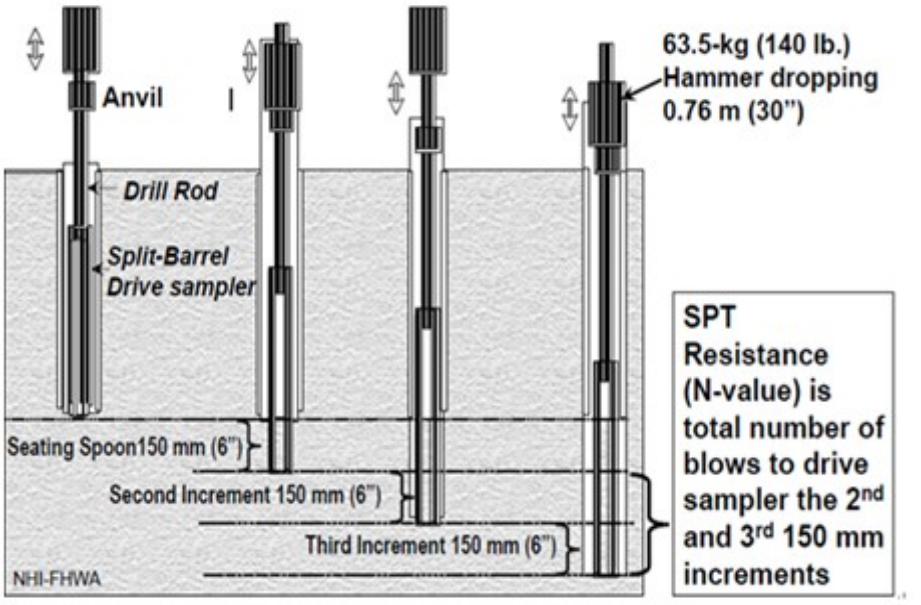

Figure 2.2 Standard Penetration Test

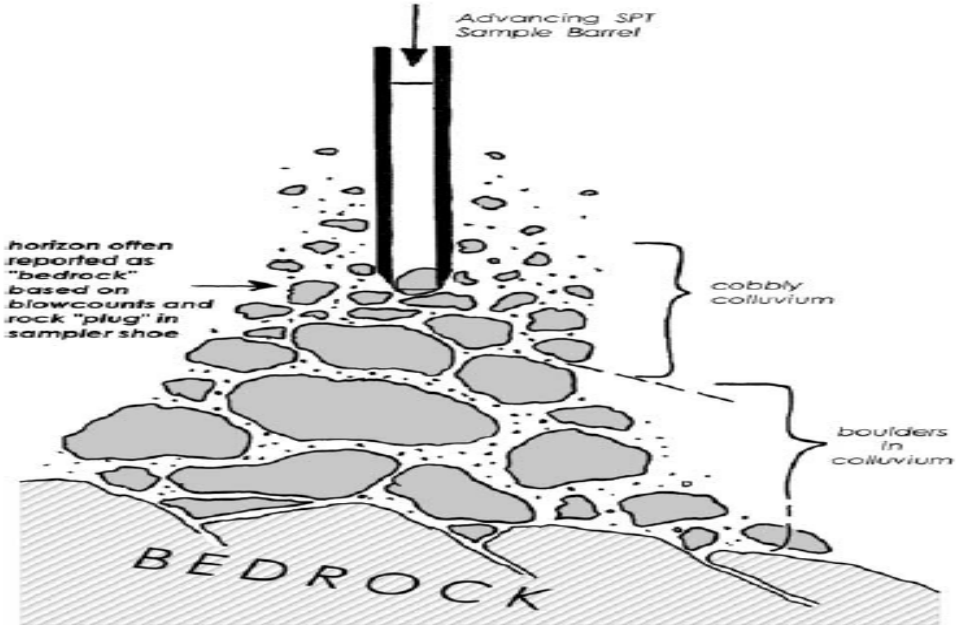

Figure 2.3 Standard Penetration Test's One Disadvantage When the Sampler Faces Bigger Rocks than the Sampler Shoes

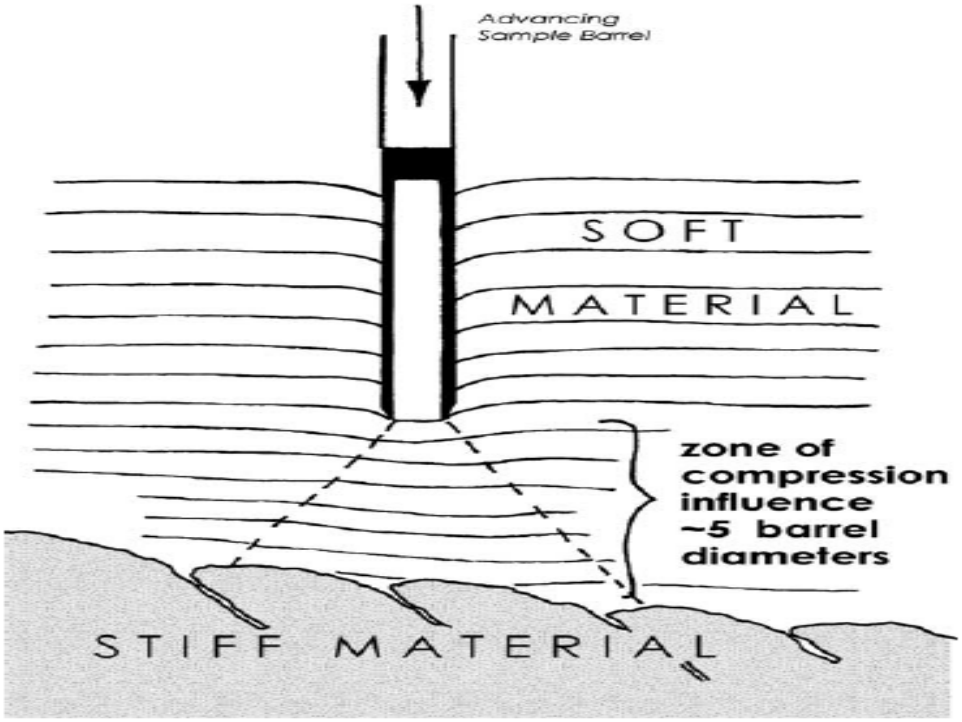

Figure 2.4 Another disadvantage of the SPT when the sample barrel in the soft material is close to the stiff material

2.3 Standard Penetration Test Correlation for Test Procedure

To boost SPT data's repeatability, the gained SPT information can be altered for many site-specific elements. Burmister's energy adjustment considered that the transferred hammer energy was 100 percent (a 140lb (63.5kg) hammer weigh multiplies dropping height 30 in (76cm) = 4200 ft-lbs uncorrected input energy). Skempton showed the steps to have a standardized blow count. He also enabled hammers of varying efficiency to be considered. Because the initial SPT hammer showed around 60 percent efficiency, this adjusted blow count is considered as "N_{60}". A donut hammer, a smooth cathead and worn hawser rope are the "standard" and this is compared to other blow count values. Safety hammers and trip releases hammer usually show higher energy ratios(ER) than 60 percent (Skempton, 1986). N_{60} is represented below

N_{60} = $(E_m * C_B * C_S * C_R * N)/0.6$

E_m = the hammer efficiency

C_B = borehole diameter correction

C_S = the sample barrel correction

C_R = the rod length correlation

N = raw spt N-value recorded in the field

Skempton made a table to get the suitable values of $C_{R,}$ C_S and C_B (Skempton, 1986) and Clayton gave a widened tabulation of SPT hammer efficiencies (E_m) (C. Clayton, 1990). D'Appolonia et al. in 1969 showed important clue that restriction developed with depth in sand and this influenced on SPT penetration significantly along with stress history (Horn, 2000). Gibbs and Holtz (1957) had offered a mean to adjust SPT N values for a "standard effective overburden" pressure N´ so that N values in identical materials at dissimilar deepness could be correlated (GIBBS, 1957). They represented $N' = C_N * N$, where N is the raw SPT blow count gained in the field and C_N represent correction factor. It is going to be explained in 2.6.3 as well.

The standard effective overburden pressure was represented as an effective stress, σ' and C_N value equals to one over the square root of σ'. When the Gibbs and Holtz overburden correction was handled to the places where samples were gained around the end of consistent soil deposits, the correction was not enough and the sample have higher N value. This is because the sampler perceives the stiffer material under the sampler as shown in the Figure 2.4. Liao and Whitman applied this overburden correction to Skempton's energy-corrected value (N_{60}) and this value showed as $(N_1)_{60}$. The $(N_1)_{60}$ consider rising confinement along the depth. The $(N_1)_{60}$ was represented below (Liao & Whitman, 1986)

$(N_1)_{60} = N_{60} * (2000\text{psf})^{0.5} / \sigma_z'$ (1psf = 47.9 pa)

Above equation, σ_z' represent vertical effective stress in the place where the sample was gained. Robertson and Wride revised Skempton's tabulation and supplemented a few correction factors that were suggested by Liao and Whitman (P. K. Robertson, Fear, Youd, & Idriss, 1997). This new tabulation is shown in the Table 2.1

Table 2.1 Corrected Standard Penetration Values (P. K. Robertson et al., 1997)

Factor	Equipment Variable	Term	Correction
Overburden pressure		C_N	$(P_a/\sigma'_{vo})^{0.5}$ but $C_N \leq 2$
Energy ratio	Donut hammer	C_E	0.5-1.0
	Safety hammer		0.7-1.2
	Automatic hammer		0.8-1.5
Borehole diameter	65-115mm	C_B	1.0
	150mm		1.05
	200mm		1.15
Rod length	3-4m	C_R	0.75
	4-6m		0.85
	6-10m		0.95
	10-30m		1.0
	>30m		< 1.0
Sampling method	Standard sampler	C_S	1.0
	Sampler without liners		1.1-1.3

The N value corrected by the overburden stress offer a constant reference value for penetration confinement. The value has been used for the assessments of liquefaction susceptibility (Youd & Idris, 1997). Robertson and Wride showed $(N_1)_{60}$ below (P. K. Robertson et al., 1997)

$$(N_1)_{60} = N*C_N*C_E*C_B*C_R*C_S$$

Above N represent the uncorrected N value, $C_N = (P_a/\sigma'_{vo})^{0.5}$ (with the confinement when $C_N \leq 2$) is the correction by effective overburden stress (Liao and Whitman, 1986), P_a is a reference pressure, 100kPa, σ'_{vo} is the vertical effective stress, $C_E = ER/0.6$ is the correction for rod energy, ER is the substantial energy ratio of the drill rig represented in percent, C_B is a correction by borehole diameter, C_R is a correction by drill rod's length, and C_S is a correction by the sampling method. From 1986 released interrelationship has more and more applied corrected $(N_1)_{60}$ values with other variables like angle of internal friction and relative density. Even though the most significant elements seem to be how the borehole is kept in steady state, $(N_1)_{60}$ values are used to assess the potential of liquefaction (HOLTZ.R.D, 2005).

2.4 Standard Penetration Test Energy Measurement

It is important to make same test results in any field or laboratory test process. In the SPT it is difficult to make same drops to keep the identical impact velocity and delivered energy, and this is the major cause of the unreliability of N value. Schmertmann and Palacios uncovered that N value is inversely corresponding to the energy gained by the soil during a test. The way to measure the energy in the rods was cultivated to know the experimental results of this type (J. H. Schmertmann & Palacios, 1979). Schmertmann et al. was the first person who tried to judge the changes directly in ram impact velocity. He measured the strain in the drill rod and computed delivered energy. He guessed that the kinetic energy of the driving system is totally moved to the drill rod before the mirrored stress wave reached back at the peak (J. Schmertmann, Smith, & Ho, 1978). Therefore, the transmitted energy is

$$E(t') = c/EA* \int_0^{t'} F(t)^2 \, dt$$

In the above equation,

c = the speed of the stress wave spread

E = the elasticity modulus of the drill rod

A = cross-sectional area

F = gauged force the around the peak of the drill rod depending on time

t´ = the time when the initial force measurement moves through zero

The major disadvantage of Schmermann's access is that before all conveyed wave has been entered the mirrored wave will reach at the peak for short drill strings. If there is not a tight link in the drill string, an early zero is attainable as well. Kovacs et al. tried to gauge the velocity of the hammer at the moment of impact. This will make it possible to measure the energy applicable before impact happens. However, these kinds of measurements do not contain energy losses at impact and do not deliver a time history record of the case (W. Kovacs, Griffith, & Evans, 1978). Thus, a mean from the pile dynamics area was applied. It is perceived that from pile dynamics the energy transferred to the rod can be represented as a function of time

$$E_i(t´)=\int_0^{t'} F(t) * v(t)dt$$

v = the velocity gauged depending on time

The quantities can be gauged through the strain gages for the force but the velocity can be gained by integration of the product of accelerometers. A force-displacement relation of the case would be usable as well. However, since the troubles connected to the acceleration record happened this mean has not succeed due to high vibration frequencies occurred from metal to metal impact (Hauge, 1979).

As a try to gauge the energy gained by the soil during an SPT, Schmertmann and Palacios applied two force transducers. One is placed at the top and the other one is placed bottom of the drill string, respectively. In this method through the force record the incident and reflected energy could be gained at the peak and lowest part. Figure 2.5 represents a simplified procedure of the hammer-impact wave pulse

shifting up and down the rods and through the two load cells (J. H. Schmertmann & Palacios, 1979).

2.4.1 Creation of Waves in the SPT Procedure

Once the hammer hit with force on the rod, it creates a compression wave moving down the rod and simultaneously a stress wave is created in the hammer. The size and form of the stress waves can be chosen by considering the velocity since the force and velocity are proportionate. Fairhurst represents what principally occurs when two identical materials hit with force. Across the touched plane two circumstances must be satisfied during impact(Fairhurst, 1961):

(1) the force in the hammer must be equal to the force in the rod

(2) when the two exteriors are contacted the absolute spatial velocities of the hitting end of the hammer and the hit end of the rod must be same all the time

From above situations the particle velocity in the rod and the hammer can be represented in the aspect of the impact velocity.

$v_h = \alpha * v/(1+\alpha)$, $v_r = v/(1+\alpha)$

v = the impact velocity

v_h = the particle velocity in the hammer

v_r = the particle velocity in the rod

α = the material ratio

2.4.2 Creation of Waves in the Rod

Using a safety hammer and AW rods, a hammer blow is considered in the SPT process now. In Figure 2.6 the hammer and the driving rod are represented with their length. To compensate for the total length for the borehole to be investigated, the AW rods are segmented in five foot and are attached by threads(Aboumatar, 1994).

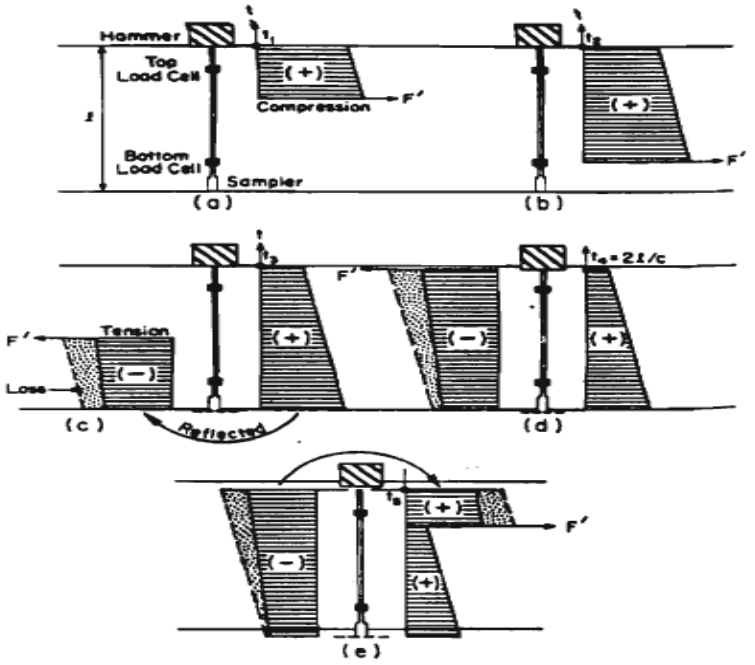

Figure 2.5 A Simplified Procedure of the Hammer-Impact Wave Pulse Shifting up and down the rods

A compression stress wave is created in the rod and it is transmitted downward with speed c. In the hammer two stress waves are produced and these waves are developed from the point A. One of the two stress waves is transmitted upward and the other wave moves downward making tension in the hammer. The distance between A and B is not long and because a free end reflection happens at B, the stresses in the part of A-B will be removed due to the superposition of waves. For pragmatic and convenience purposes, one can disregard the section A-B and say a tension wave is created moving down the hammer (Aboumatar, 1994).

The wave spread in the structure is represented in Figure 2.8 and Figure 2.9. The hammer and the drive rod consist of the same material and this represents that the material ratio α is equals to the ratio between the areas. In this case the ratio is 0.3. From the equation introduced above the particle velocity in the drive rod v_r would be 0.77v. Before impact, the particle velocity in the hammer equals the impact velocity. As shown in the Figure 2.8b in order to have the same particle velocity in the hammer and in the rod which is 0.77v, at impact this velocity will

be reduced by 0.23v by using the equation mentioned above to obtain particle velocity in the hammer. The identical values would show the stresses. A free end reflection happens when the tension wave moving downwards arrive the end of the hammer D (Aboumatar, 1994).

The extra mass at the end of the hammer is very small when it is compared to the hammer weight and the stress because of the inertia forces of this mass, so the additional mass at the bottom of the hammer is insignificant. This tension wave mirrors as a compression wave of same size and this compression wave remove the oncoming tension wave (Figure 2.8c). At the point E in the middle from the drive rod and the AW-rods, approaching wave detects a reduced area. The two rods are identical material so that the material ratio α is equal to the ratio in the middle from the areas and the value is 0.457 (Aboumatar, 1994).

This leads to a reflection and transmission of waves in accordance with below equations and these equations produce 63 percent of the compression wave force transferred and 37 percent mirrored back up as tension. By using the below equations the transferred particle velocity is $1.373v_i$ and in this situation v_i is v_r that is 0.77v (Figure 2.9d). The transferred wave spreads down the rod and confronts the transducers that are away six inches below linked point E. A newly changed area is detected at the joint in the middle from the two AW-rods. However, the change is so small and the small change leads to the disturbance that influences on the minimum wave transmission. When the wave traveling down arrive the end of the rod (Figure 2.7c), it is mirrored in accordance with the boundary condition and moves backwards the rod. The transducers feel the wave again and it moves to juncture E(Aboumatar, 1994).

$F_t = 2\alpha * F_i/(1+ \alpha)$, $V_t = 2 * v_i/(1+ \alpha)$

$F_r = -(1- \alpha) * F_i/(1+ \alpha)$, $V_r = -(1- \alpha) * v_i/(1+ \alpha)$

From the above equations,

v_t is the velocity in the transmitted wave and F_r is the force in the transmitted wave. v_r is the velocity in the reflected wave and F_r is the force in the reflected wave. v_i is the velocity in the incident wave and the F_i is the force in the incident wave.

The transferred wave to the drive rod is in tension and the wave value through the equation for the particle velocity in the rod is 0.148σ. The downward mirrored wave in the hammer is in tension and the value is 0.08σ (Figure 2.9e). After that happens, the reflected wave at the juncture E will arrive point A and then transmission and reflection happen again (Aboumatar, 1994).

Through the equation for v_h and v_r, the reflected and the transmitted waves are in tension and values of them are 0.185σ and 0.102σ. The traveling tension waves in up and down superimpose on each other to yield a sum value, 0.62σ. The initial downward traveling compression wave is 0.77σ, this value will decrease by 0.62σ and as a result a downward traveling compression wave is 0.15σ (Aboumatar, 1994).

Transmission and reflection happens again at the point E. The following transferred wave is still in compression and the value is 0.206σ. The descending tension wave is 0.185σ and the value is mirrored as a compression wave value, 0.07σ. Just before the tension wave is mirrored on the top it travels up the rod. When it attains the juncture E, the tension wave rerun the cycle of reflection and transmission as explained above (Aboumatar, 1994).

A number of small reflections and transmissions will happen in the top and the end areas since the unevenness in the hammer geometry can be seen at the top and at the end. A detailed explanation of the wave spread in the hammer is quite discouraged and confused because of these truths. In some situations superposition of waves will cause to remove their impact and considering the waves created in the hammer longer than the 2L/c period of the hammer is not necessary. Impacts and reflections will lead to losses in wave intensity (Aboumatar, 1994).

Therefore, in the hammer the whole result of waves will decrease very quickly. The transducers feel the signals and they always depend on the superposition of waves going by this part. Through part E when the downwards transferred wave goes by the transducers a blow will be initially perceived (Aboumatar, 1994).

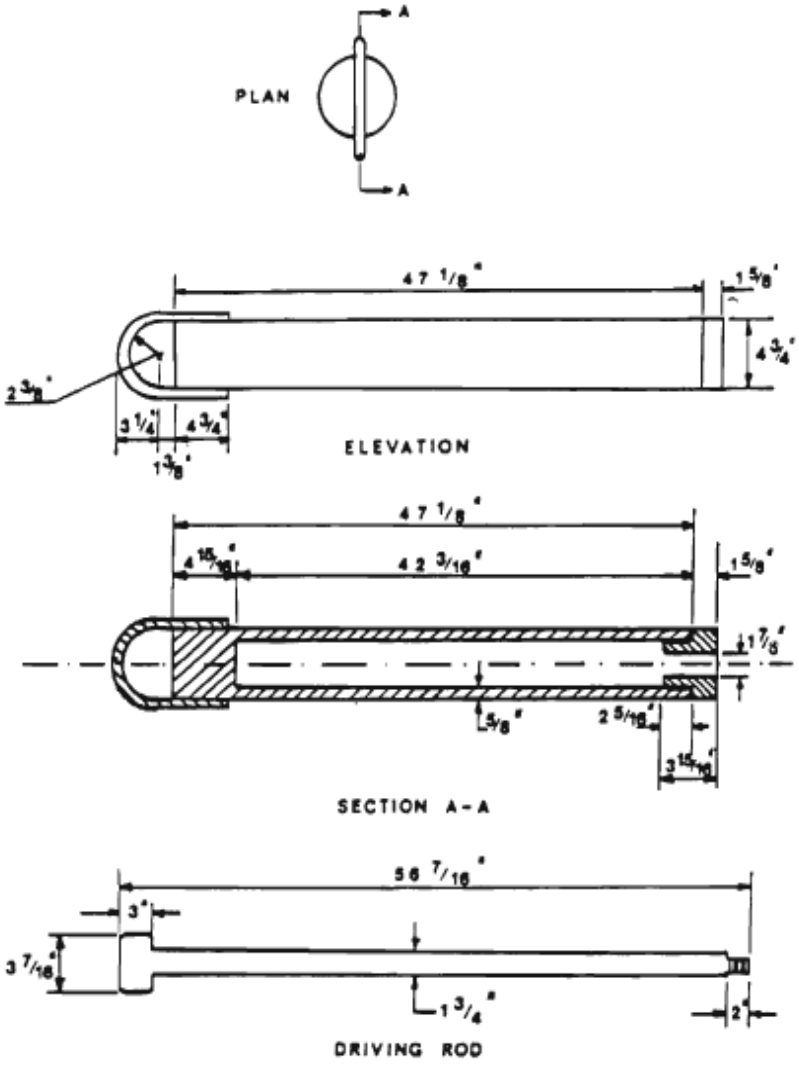

Figure 2.6 Safety Hammer and Driving Rod with their Lengths

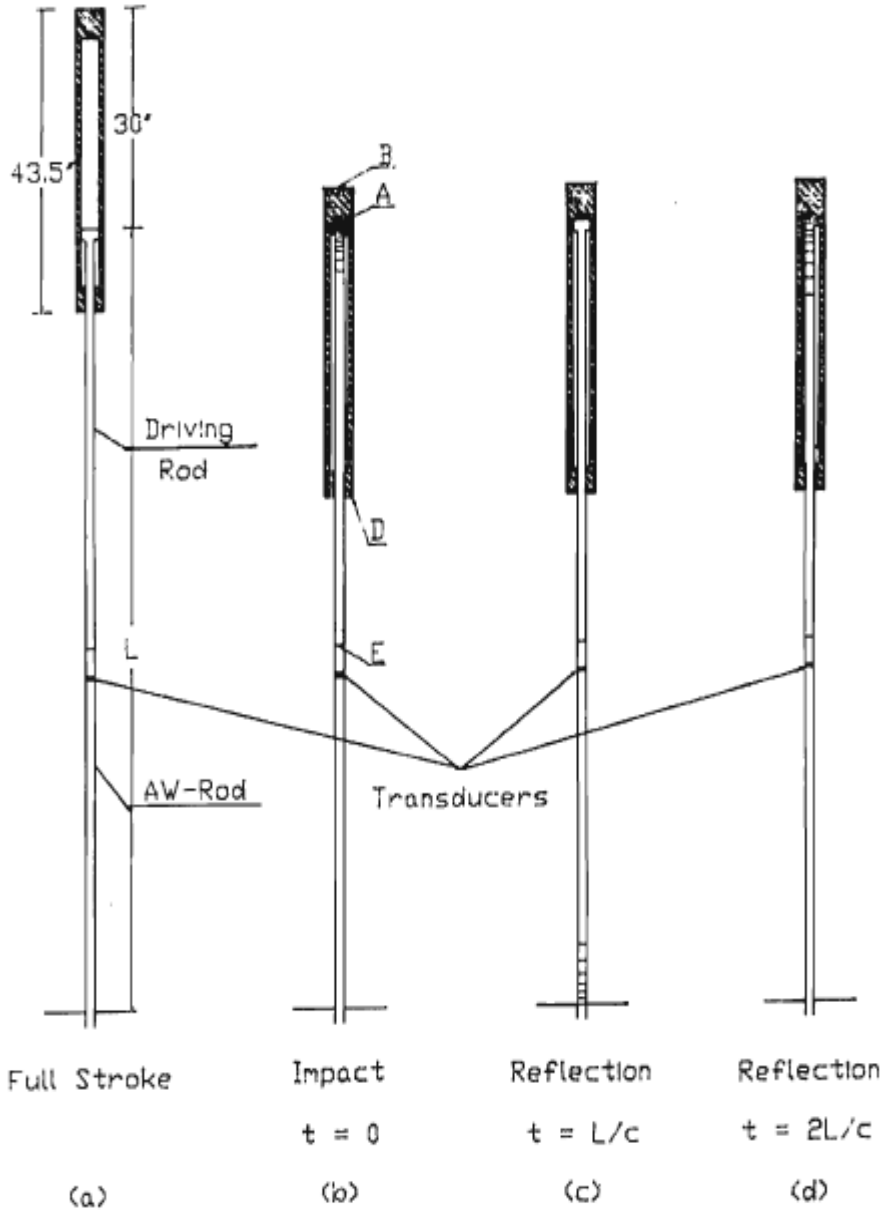

Figure 2.7 Diagram of a Blow in the SPT with Safety Hammer

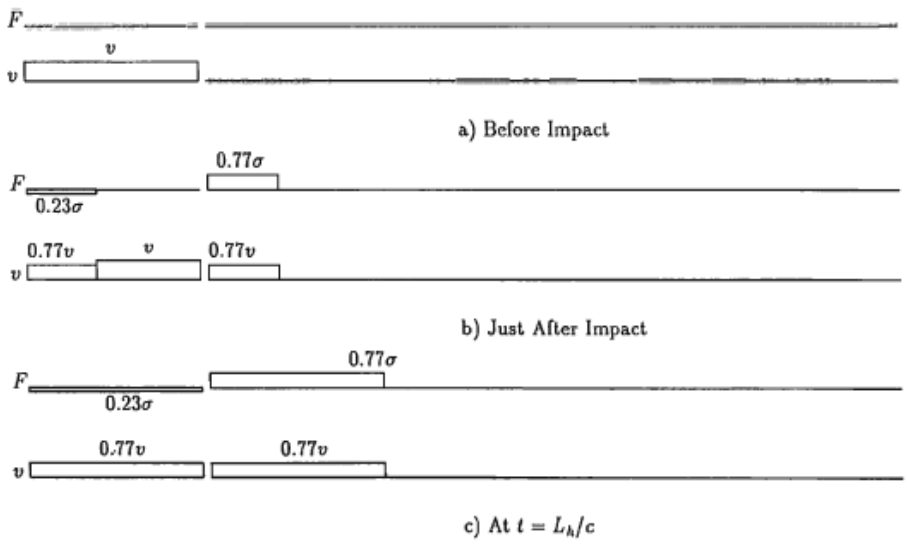

Figure 2.8 Wave Movement in the Safety Hammer

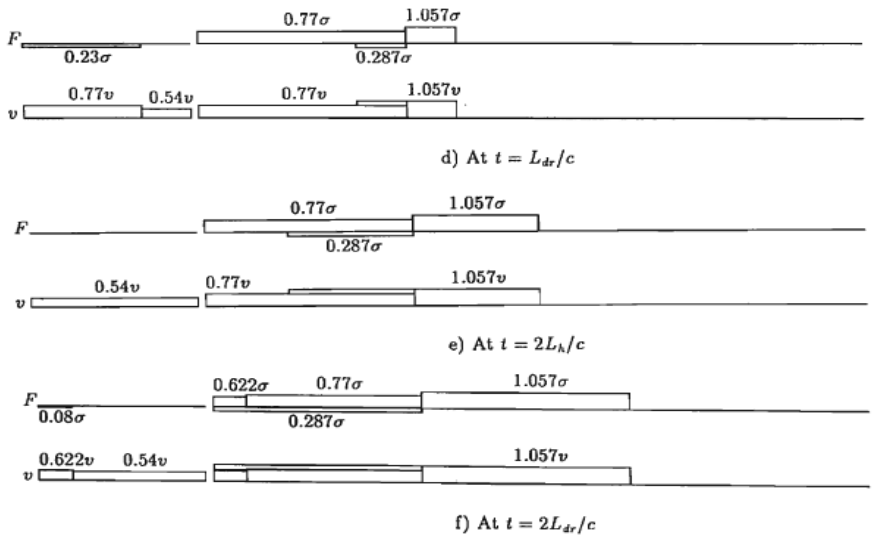

Figure 2.9 Continued Wave Movement in the Safety Hammer

A reflection from the peak or from the end will reach the spot of transducers relying on the length of rods and strength of signals will be superimposed on the ones presented. In a 20 ft (609.6cm) height rod the transducers feel a theoretical predicted wave and this is presented in Figure 2.10 with a line of velocity and stress waves that are gained from experimental information (Aboumatar, 1994).

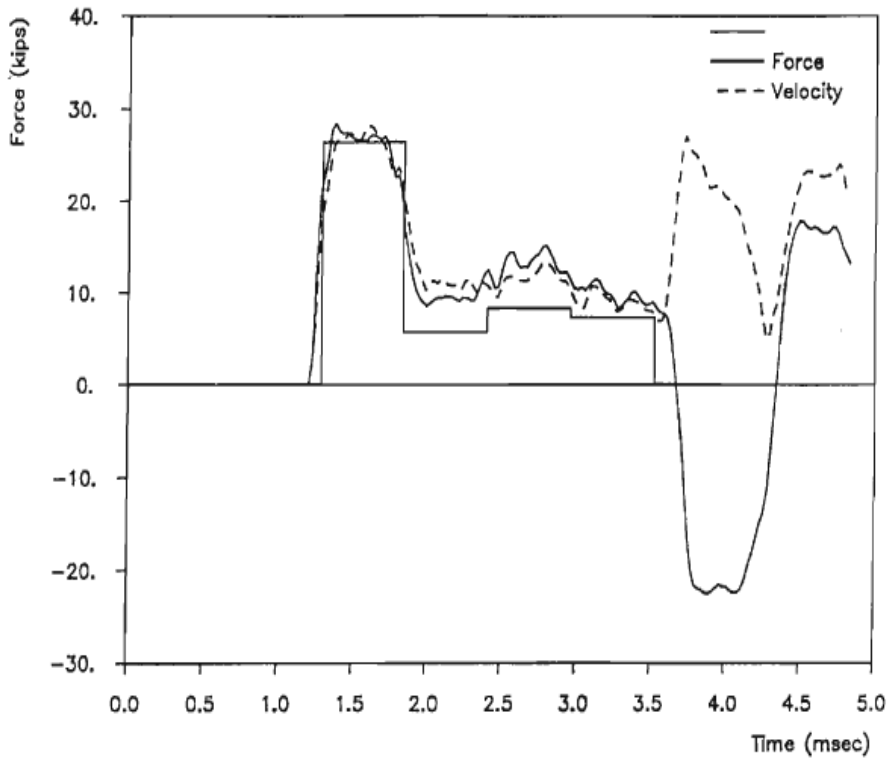

Figure 2.10 Wave Movement Values from the Theory and the Experimental Data

2.5 Factors Affecting the N Values

Table 2.2 Factors Influencing N Values (Navy, 1986)

Factors	Effects

Insufficient cleaning of hole	SPT is conducted in loose slough. Sludge may be trapped in the sampler and may be compressed as sampler is driven, reducing recovery
Not placing the sampler spoon on undisturbed substances	Inaccurate blow counts are gained
Sample spoon's pushing above the lowest part of the casing	Blow count is improved in sands and is diminished in cohesive soils
Not succeeding to keep adequate head of water in borehole	The water table in the borehole at the minimum must equal to the piezometric height in the sand, or the lowest part of the borehole may be changed into a loose state reducing N values.
Stance of the person who operate the SPT	N values for the same soil can be various relying on who perform the rig and way of operator
Overdrive sampler	Larger N values are the result of overdriven sampler
Clogged sampler by gravel	Larger N values are gained when the sampler is clogged by gravel
Clogged casing	Large N value may be gained for loose sand when it is sampled below groundwater table. Sand rise and clog casing due to hydrostatic pressure
Before casing overwashing	Low N value may be result for dense sand because overwashing loosens sand
Drilling method	Depending on drilling methods such as cased holes or mud stabilized holes, different blow counts may be gained for the same soil

Using the non-standard hammer drop	Transferred energy per blow is not consistent. North America and European countries use different hammers
Free fall of the drive weight is not achieved	Applying more than 1-1/2 turns of rope around drum or applying wire cable will make the free fall of the drive weight restricted
Not adopted accurate weight	Driller often uses drive hammer but weights of it vary from the standard by 10lb(4.54kg)
Hammer does not hit the drive cap with concentration	Impact energy is diminished and blow count increases
Adopting a non-guide rod	Inaccurate blow count is gained
Adopting a bad tip on the sampling spoon	If the tip is impaired or raise the end area, blow count can increase
Use drill rods that have more weight than that of standard	When the rods weight a lot, more energy is gained and N value increases
Not containing the adequate N values and penetration	Wrong N values are gained
Not exact drilling process	During drilling process, the soil is disturbed and N value will be affected (For example, drilling with cable tool)
Too large drill holes	Holes that are larger than 10 cm in diameter area are not approved. Larger diameter holes may cause decreased N value
Not suitable supervision	A sampler is often obstructed by gravel or cobbles so that the N value is suddenly raised. Inexperienced supervisor dose not catch this.

Not adequate soils' logging	The sample is not appropriately explained
Too big a pump	If a pump has high capability, it will loosen the soil at the bottom of the hole and this lead to a decrease of N value

2.6 Standard Penetration Test Influence Factors in Granular Soil

2.6.1 Ageing

Chosen data for field and laboratory tests indicate that the correlation among blow count, effective overburden pressure σ_v'(kg/cm2) and relative density D_r is approximately represented by an equation by Meyerhof: $N_{60}=(a+b*\sigma_v')*D_r^2$ or $(N_1)_{60} = (a+b)*D_r^2$. In this equation a and b are constants for a certain sand within the range $0.35<\sigma_v'<0.85$ and $0.5kg/cm^2<\sigma_v'<2.5kg/cm^2$. The values of a and b are be apt to rise with rising grain size, with rising age of the deposit and with rising overconsolidation ratio. By considering the influences of differing rod energy ratios and of ageing, the continuous and obvious discrepancy between field and laboratory test results are solved. Ordinary outcome in the ageing effect for normally consolidated fine sands are represented in below Table 2.3 (Skempton, 1986)

Table 2.3 Ageing Effect

	Age: years	$(N_1)_{60}/D_r^2$
Laboratory tests	10^{-2}	35
Recent fills	10	40
Natural deposits	$>10^2$	55

2.6.2 Overconsolidation

K_{ONC} is the in-situ stress ratio between vertical and horizontal effective stress in normally consolidated sand and K_O is the in-situ stress ratio between vertical and horizontal effective stress in overconsolidated sand. If K_{ONC} has an overconsolidation ratio OCR of 1.0, the identical sand when overconsolidated (OCR>1) will have an raised blow count (Skempton, 1986).

$K_O = \sigma_h' / \sigma_v'$

Experiment results in Figure 2.11 from Marcuson and Bieganousky explains the correlation between N value and overconsolidation ratio (OCR). When overconsolidation ratio (OCR) = 3 compared with the same sand at OCR =1, remarkable increased N value is gained (Bieganousky & Marcuson, 1976). From above, it appears that in-situ horizontal stresses play an important role in determining N value.

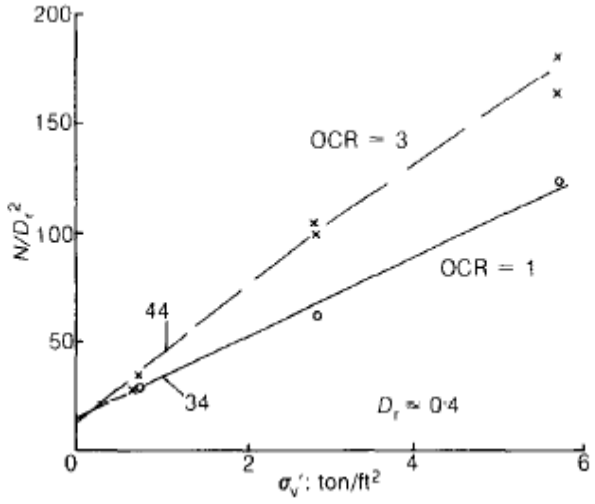

Figure 2.11 Overconsolidation Influence

2.6.3 Overburden Pressure

Gibbs and Holtz (1957) had offered a mean to adjust SPT N values for a "standard effective overburden" pressure N´ so that N values in identical materials at dissimilar deepness could be correlated (GIBBS, 1957). They represented $N' = C_N * N$ and now if $N/D_r^2 = (a+b*\sigma_v')$, $C_N = (a/b+1)/(a/b+\sigma_v')$. a/b is ranged from 1.0 for fine sands of medium

relative density to 2.0 for dense coarse sands when sands are normally consolidated and C_N value (Figure 2.12) is represented (Skempton, 1986).

2.6.4 Relative Density and Particle Size

The analysis of the SPT test results in cohesionless soils has focused on correlations with relative density (D_r). Marcuson et al. make a conclusion that the SPT is not exact enough to be suggested for the relative density at a spot if the spot does not have any other correlations (MARCUSON, 1978). N value should be corrected to $(N_1)_{60}$ to gain relative density. Skempton proposes that it is adequate to presume the equations below for relatively recently deposited normally consolidated sand. N value increases with increasing particle size from the Table 2.4 (Skempton, 1986).

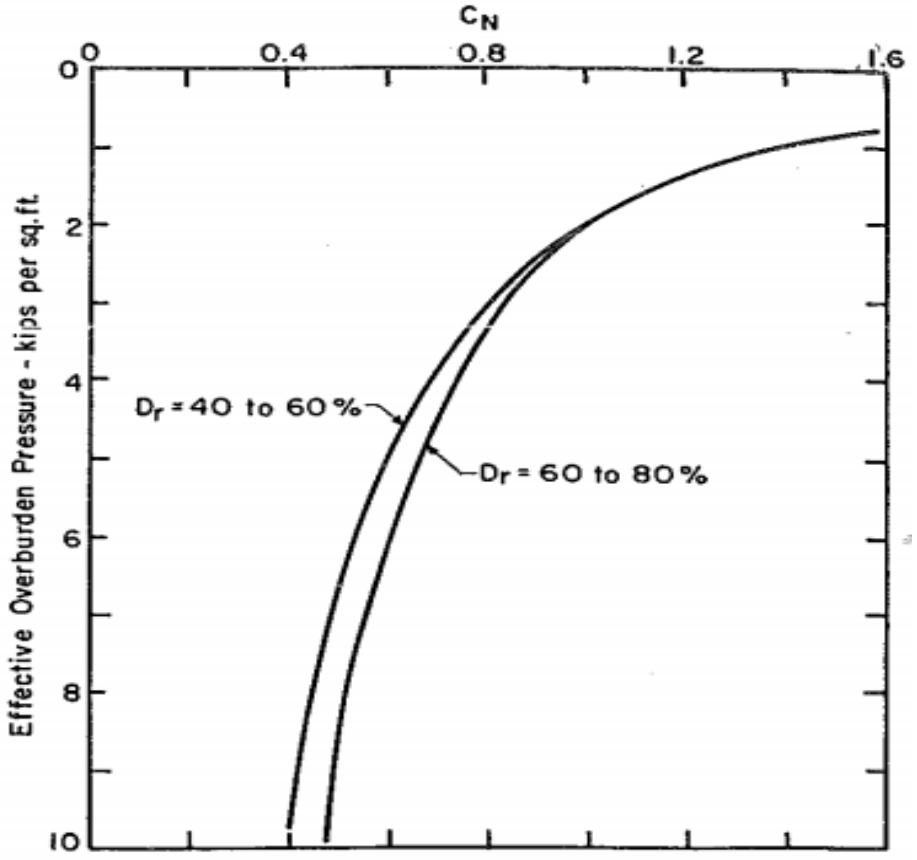

Figure 2.12 C_N Values Depending on the σ_v' and D_r (Bolton Seed, Tokimatsu, Harder, & Chung, 1985)

$(N_1)_{60}/D_r^2 = 60$

D_r = relative density of sand.

Table 2.4 Relation between D_r and $(N_1)_{60}$ (Skempton, 1986)

Classification	D_r(%)	$(N_1)_{60}$ (blows/300mm)
Very loose	0-15	0-3
Loose	15-35	3-8
Medium	35-65	8-25
Dense	65-85	25-42
Very dense	85-100	42-58

2.6.5 Fiction Angle

Various correlations have been cultivated to gain the friction angle (φ') of sands through the relation between a blow count and relative density. De Mello, however, uses the SPT with caution to guess D_r and he uses the value from the SPT to have relation between D_r and φ' (De Mello, 1971). The correlation among φ', N and vertical effective overburden pressure (σ_v') grown by De Mello (1971) for granular soils is on the basis of the experimental results from Gibbs and Holtz (1957). This was confirmed with other data and it was acceptable when this was used for SPT outcomes about quite shallow depth that is no more and equal to 2m (P. K. Robertson, 1986). Below Figure 2.13 shows that the N value increases with increasing φ' when σ_v' value is same.

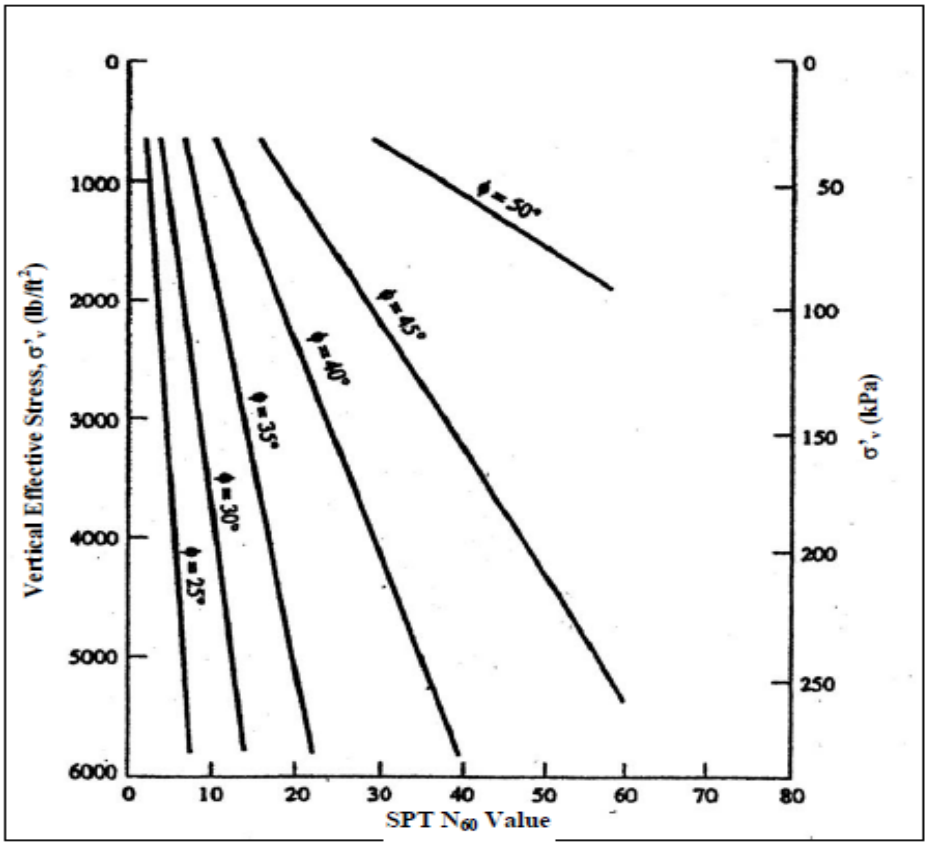

Figure 2.13 Correlation between φ' and N_{60} (De Mello, 1971)

2.7 Standard Penetration Test Influence Factors in Cohesive Soils

2.7.1 Correlation between N Value and Undrained Shear Strength

Ladd et al. (1977) propose that if the clay is not relatively hard and insensitive, undrained shear strength, S_u, from SPT N-value is useless in cohesive soils. After C_u value is gained from SPT, the value should always be checked again through the laboratory tests on the samples (Ladd, 1977). Below Figure 2.14 shows the relation between C_u and SPT N-value. N-value increases with increasing C_u value in all soil types.

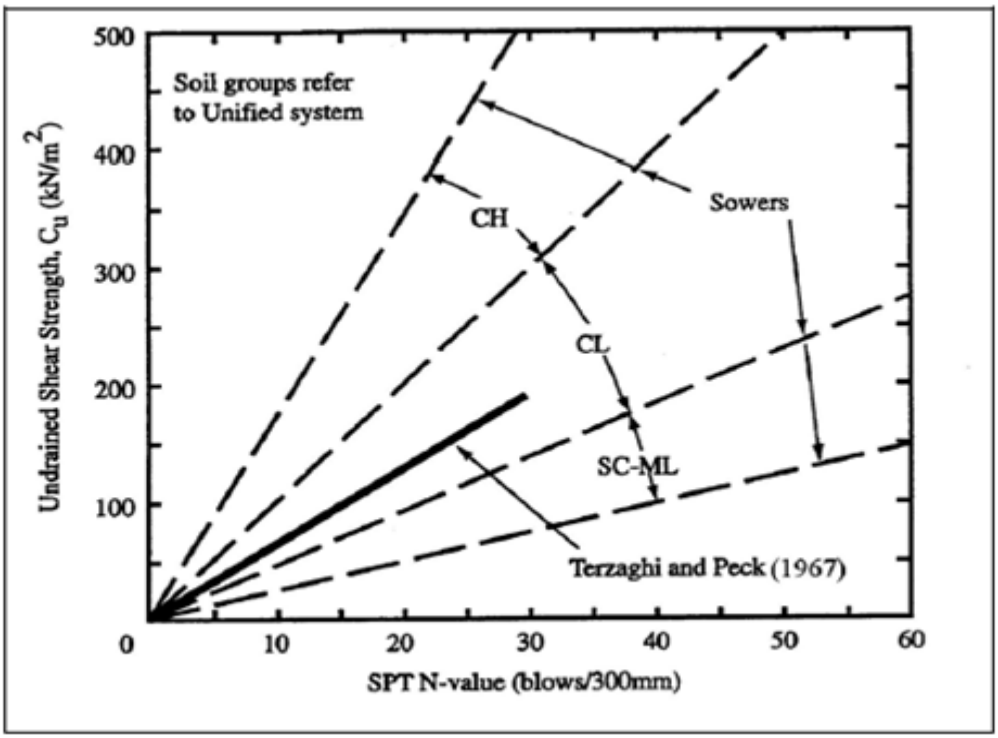

Figure 2.14 Correlation between N value and S_u (Sowers, 1979)(Table A-4)

2.8 Application of Standard Penetration Test

2.8.1 Soil Profile

To find the borders between kinds of rocks or dissimilar soils, profiling is executed. Dynamic penetrometers of different extent of dimensions are handled to have approximate estimations of penetration resistance at dissimilar deepness and locations across a site. When the SPT is employed in the role of a dynamic penetrometer, it will be often executed at 1 m centers in each borehole (Zhang, 2009) and how it is used for soil profile is shown in Figure A-2.

2.8.2 Soil Classification

Soil classification is the act processed during ground investigation to separate soils and rocks into a few bands and each band includes materials expected to conduct extensively similar engineering action. The engineering parameters are most important to estimate behavior of mate-

rials and the parameters are strength, compressibility and permeability and rate of consolidation. The most normally adopted means for classification are sample description, moisture content and plasticity testing (for cohesive soils) and particle size distribution (for granular soils). Because SPT connects with a sampler and a penetrometer, it is attainable to make the classification with the SPT (Zhang, 2009).

Table 2.5 Classification of Soils and Rocks from SPT

Sands	$(N_1)_{60}$ 0-3	Very loose
	3-8	Loose
	8-25	Medium
	25-42	Dense
	42-58	Very dense
Clays	N_{60} 0-4	Very soft
	4-8	Soft
	8-15	Firm
	15-30	Stiff
	30-60	Very stiff
	> 60	Hard
Weak rock (except chalk)	N_{60} 0-80	Very weak
	80-200	Weak
	> 200	Moderately weak to very strong

Chalk	N_{60} 0 -25	Very weak
	25-100	Weak
	100-250	Moderately weak
	> 250	Moderately strong to very strong

Note

N_1 : Corrected N value by 100 kPa effective overburden pressure

N_{60} : Corrected N value by 60 percent of theoretical free-fall hammer energy

$(N_1)_{60}$: Corrected N value by vertical effective stress and input energy

2.9 Indirect Application of Standard Penetration Test

2.9.1 Young's Modulus and the Coefficient of Volume Compressibility

Soil stiffness is directly affected by connections of state (bonding, fabric, degree of cementation, stress level), strain level (and effects of destructuration), stress history and stress path, time-dependent effects (ageing and creep) and kind of loading (monotonic or dynamic). From these intricate interactions, the distinguishing response of clay concerning small strain stiffness and stiffness non-linearity should firstly be determined in situ seismic techniques or laboratory tests (Schnaid, 2009).

The SPT is a normal site investigation method to determine soil stiffness in a lot of countries. In order to approximately calculate the coefficient of volume compressibility, m_v, and the undrained Young´s modulus of stiff overconsolidated clays, E_u, various empirical correlations have been introduced and are recently selected for engineering practice (Schnaid, 2009). The coefficient of volume compressibility, m_v, is employed to calculate settlements for clays soils and can be gained through below equations (Butler, 1974):

$m_v = 1/f_2 * N$ (m^2/MN)

f_2 is gained from below Figure 2.15. When N-values decrease, m_v values have tendency to increase.

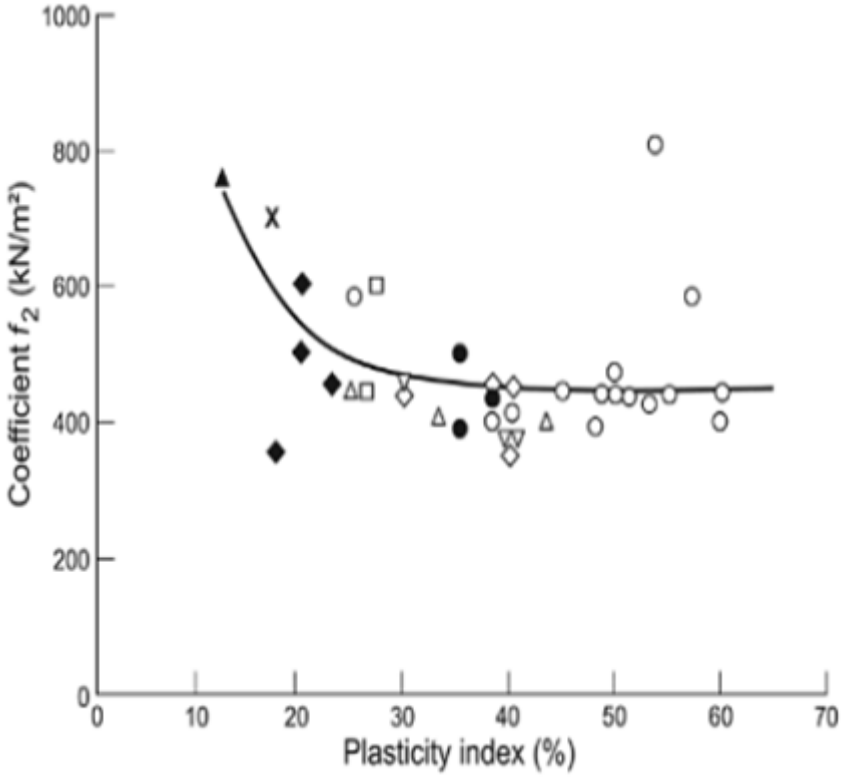

Figure 2.15 Correlation between Coefficient f_2 and Plasticitiy Index (Stroud, 1974) (Butler, 1974)

The Young´s modulus changes considerably between small strain and large strain applications. Below Table 2.6 shows the correlations between Young´s modulus and N-value depending on the soil types (C. R. Clayton, 1995).

- $E_u/N = 1$ is suitable for footings.
- For rafts where smaller movements happen $E_u/N = 2$
- For significant small strain movements for friction piles $E_u/N = 3$

Table 2.6 the Correlations between Young´s Modulus and N-value Depending on the Soil Types

Material	E´/N (MPa)	E_u/N(MPa)
Clay	0.6 to 0.7	1.0 to 1.2
	0.9 for q/q_{ult} =0.4 to 0.1	6.3 to 10.4 for small strain values (q/q_{ult} < 0.1)
Weak rocks	0.5 to 2.0 for N_{60}	

2.9.2 Shear Modulus

Shear modulus is closely related with N-values of the standard penetration test for smaller shear strains. Not considering soil kinds and deepness from ground level, the relation between N value and shear modulus may be roughly represented like $G=1200*N^{0.8}$(tons/meter^2). Much research has been done about the relation between the shear modulus and N values (IWASAKI, 1973).

Kanai et al. represented the relations as shown in Figure 2.16 mainly through the outcomes of microtremor methods. In the primary paper the Y axis are presented with respect to shear wave velocities but the ordinate are replaced with shear modulus in Figure 2.16 and it is considered that unit weights of clay and sand, respectively are 1.50 and 1.86 tons/cu.meter. Kanai's representation is characterized by a clear distinction between sand and clay (Kanai, Tanaka, Morishita, & Osada, 1967).

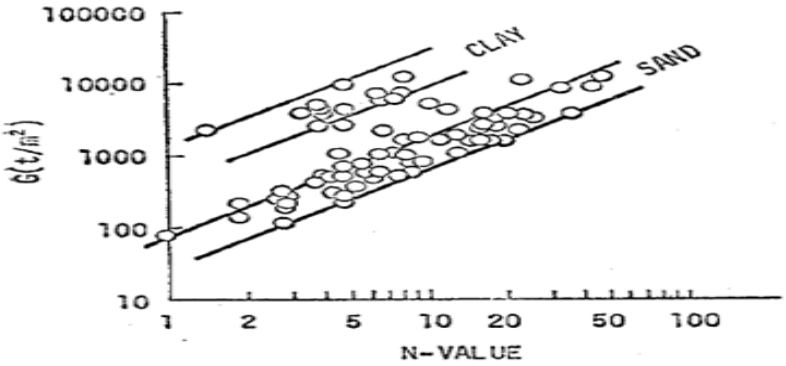

Figure 2.16 Correlation between Shear Modulus and N-value (Kanai et al., 1967)

2.10 Direct Application of Standard Penetration Test

2.10.1 Design of Piles – Shaft Resistance

The shaft resistance f_s is expressed with α, β and N values. Each parameter α and β (or K and δ) is normally gained through empirical correlations (depending on soil, pile type and construction method) although the effective stress β approach is basically safe. The correlations between f_s and N value are shown in Table 2.7 and $f_s = \alpha + \beta * N(kN/m^2)$ is used to obtain shaft resistance (Poulos, 1989).

Table 2.7 Correlation between f_s and N Value

Pile type	Soil type	α	β	Remarks	Reference
Driven displacement	Cohesionless	0	2.0	f_s=average value over shaft $\bar{N}$ = average SPT along shaft Halve f_s for small displacement pile	(Meyerhof, 1956) (Shioi & Fukui, 1982)
	Cohesionless and cohesive	10	3.3	Pile type not indicated $3 \le N \le 50$ f_s is not larger than $170kN/m^2$	(Decourt, 1982)
	Cohesive	0	10		(Shioi & Fukui, 1982)
Cast in place	Cohesionless	30	2.0	f_s is not larger than $200kN/m^2$	(Yamashita, Tomono, & Kakurai, 1987)
		0	5.0		(Shioi & Fukui, 1982)

	Cohesive	0 0	5.0 10.0	f_s is not larger than 150kN/m^2	(Yamashita et al., 1987) (Shioi & Fukui, 1982)
Bored	Cohesionless	0 0	1.0 3.3		(Findlay, 1984), (Shioi & Fukui, 1982) (Wright & Reese, 1979)
	Cohesive	0 10	5.0 3.3	Piles cast under pentonite N is not larger than 3 and not smaller than 50 f_s is not larger than 170 kN/m^2	(Shioi & Fukui, 1982) (Decourt, 1982)
	Chalk	125	12.5	N is larger than 15 and smaller than 30 f_s is not larger than 250 kN/m^2	After (Fletcher & Mizon, 1983)

2.10.2 Design of Piles – Toe Resistance

The standard penetration resistance is used for toe resistance in the design of piles. Below Table 2.8 indicates several experimental interrelationships between f_b and blow counts around the end of pile. The correlations show that driven piles grow a substantially larger end-bearing resistance than bored or cast-in-place piles do. Toe resistance is obtained by using the equation f_b=K*N MN/m^2(Poulos, 1989).

Table 2.8 Correlation between f_b and Blow Count (f_b=K*N MN/m^2)

Pile type	Soil type	K	Remarks	Reference
Driven displacement	Sand	0.45	N= Mean blow count in regional failure area	(Martin, Seli, Powell, & Bertoulin, 1987)
	Sand	0.4		(Decourt, 1982)
	Silt, sandy silt	0.35		(Martin et al., 1987)
	Glacial coarse to fine silt deposits	0.25		(Thorburn & Mac Vicar, 1971)
	Residual sand silts	0.25		(Decourt, 1982)
	Residual clay silts	0.2		(Decourt, 1982)
	Clay	0.2		(Martin et al., 1987)
		0.12		(Decourt, 1982)
	Every soils	0.3	When L/d is larger than or equal to 5 (d=diameter of pile and L =length of pile) However, if L/d is smaller than 5, K = 0.06*L/d (open-ended piles) or K = 0.1 +0.04*L/d (closed-ended piles)	(Shioi & Fukui, 1982)

Cast in place	Cohesionless	0.15	f_b equals to 3.0 MN/m^2 f_b is not larger than 7.5 MN/m^2	(Shioi & Fukui, 1982) (Yamashita et al., 1987)
	Cohesive	—	f_b=0.09*(1+0.16*z) and z means tip depth and unit is m	(Yamashita et al., 1987)
Bored	Sand	0.1		(Shioi & Fukui, 1982)
	Clay	0.15		(Shioi & Fukui, 1982)
	Chalk	0.25	N < 30	(Hobbs, 1977)
		0.20	N > 40	

2.10.3 Liquefaction Potential in Granular Soils

On the basis of SPT the standards to assess a liquefaction resistance have been developed for long years. The standards are demonstrated in the below Figure 2.17 where the Cyclic Stress Ratio (CSR) versus $(N_1)_{60}$ are produced, the blow count is normalized about overburden pressure 100kPa and a hammer energy ratio is 60 percent. Below Figure 2.17 shows a graph about computed CSR and correlating $(N_1)_{60}$ information from areas where after previous almost 7.5 magnitude earthquakes, liquefaction influences were or were not monitored (Youd et al., 2001).

The Cyclic Resistance Ratio (CRR) bending line in the graph was conservatively located to divide the parts with data that show liquefaction and parts with data that show non-liquefaction. Bending lines for granular soils grew with the fine contents of 5 percent, 15 percent and 35 per-

cent as indicated in the Figure 2.17. The CRR bending line for fines contents lower than 5 percent is the fundamental penetration standard for the less complicated process and is named the "SPT clean-sand base curve." The CRR bending lines in below Figure 2.17 are useful only for earthquakes with magnitudes of 7.5 (Youd et al., 2001).

At the University of Texas, A. F. Rauch approximately represented the clean-sand base curve in Figure 2.17 through the below equation (Rauch, 1998):

$$CRR_{7.5} = \frac{1}{34-(N1)60} + \frac{(N1)60}{135} + \frac{50}{[10*(N1)60+45)]^2} - \frac{1}{200}$$

Above mentioned equation is available when $(N_1)_{60}$ is smaller than 30. When $(N_1)_{60}$ is larger than and equal to 30, soils are massive so that they cannot be liquefied. The equation may be adopted for other analytical methods in order to roughly express the SPT clean-sand base curve for normal engineering computations (Rauch, 1998).

Effect of Fines Content

Seed et al. focused on the clear rise of CRR with raised fines contents in the initial growth. It is not clear if an increase of liquefaction or a decrease of penetration resistance leads to this increase. Seed et al. made the CRR bending lines grown for diverse fines contents represented in Figure 2.17 depending on the experimental useful information (Bolton Seed et al., 1985). In Work-shop that held in 1996 sponsored by the National Center for Earthquake Engineering Research (NCEER), attendants made a newly changed correction for fines content (FC) grown to correspond to experimental database well and to help calculations with spreadsheets well. In order to roughly correct the effect of fines content (FC) in CRR the attendants suggest two equations that show below. Other parameters like soil plasticity may have an influence on fines content and liquefaction resistance but the corrections for these elements have not been grown, although the corrections are broadly adopted. Corrections should be applied with engineering caution and decision depending on only fines content. I.M.Idriss made the below equations grown with the help of R.B.Seed for adjustment of $(N_1)_{60}$ to the corresponding clean sand value, $(N_1)_{60cs}$ (Idriss, 1990):

$$(N_1)_{60cs} = \alpha + \beta^*(N_1)_{60}$$

In the above equation, both coefficients are gained through the below relations.

α =0 when Fine Contents (FC) is less than and equal to 5 percent.

$\alpha = \exp[1.76-(190/FC^2)]$ when FC is smaller than 35 percent and larger than 5 percent.

α = 5.0 when FC is larger than and equal to 35 percent.

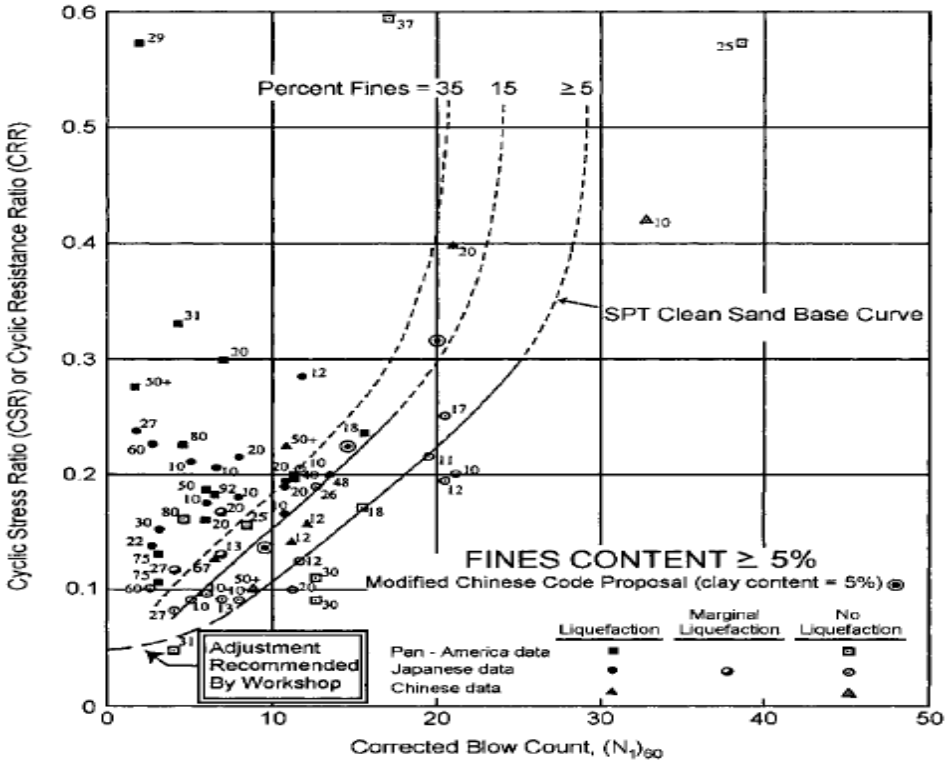

Figure 2.17 SPT Clean Sand Base Curve with Liquefactional Historical Data (Bolton Seed et al., 1985)

β = 1.0 when FC is smaller than and equal to 5 percent.

$\beta = [0.99 + (FC^{1.5}/1000)]$ when FC is smaller than 35 percent and larger than 5 percent.

$\beta = 1.2$ when FC is larger than and equal to 35 percent.

The above mentioned equations may be used to compute the normal liquefaction resistance. We can guess if a place has liquefaction potential with the above equation and Figure 2.17 (Youd et al., 2001).

3 Cone Penetration Test

3.1 Introduction of Cone Penetration Test

The Cone Penetration Test, called simply as CPT, is executed by pushing 60° cone by a water pressure. The cone has a face area of $10cm^2$(35.7mm diameter) and move with a steady speed (2±0.5cm/s) while measuring needed force to do so. A friction cone is most usually adopted. The sleeve area is $150cm^2$ with the identical exterior diameter as the cone. The sleeve is closely placed in higher part of the cone and shear force on the friction sleeve is gauged (C.R.I. Clayton, 1995).

Electrical and mechanical methods to gauge side friction and cone resistance are recently employed. The cone has different shape depending on the employed means. The cone moves down the ground level without borehole, adopting unique mobile penetrometer rig that is moved by water pressure. The CPT was grown in Netherland in the 1930's and it was primary used to discover and assess the density of soil layers under the soft deltaic clays in this country in order to design driven pile. The primary cone and the mechanical Delft cone is illustrated in the below Figure 3.1. The cone improved in the Delft Laboratory for Soil Mechanics is used over the Netherland and in many other countries (C.R.I. Clayton, 1995).

The original cone had the problem and it is that the soil particles are firmly stuck between the cone and end side of the rods. The problem was solved by the Delft cone. Begemann firstly brought the mechanical friction cone (Figure 3.2) in higher position of the Delft mantle and the value of Delft cone was considerably improved by him (Begemann, 1965).

The electric cone shown in Figure 3.3 was originally made in 1948 and the measurements carry out through strain gauges or transducers in higher part close to the cone, but it became widely used in the end of 1960s. When cone go through the ground, the advanced measurements of the pore pressure primary happened in the end of 1960s and in the beginning of 1970s. Cone has been advanced more and it is still persisted in these days (C.R.I. Clayton, 1995).

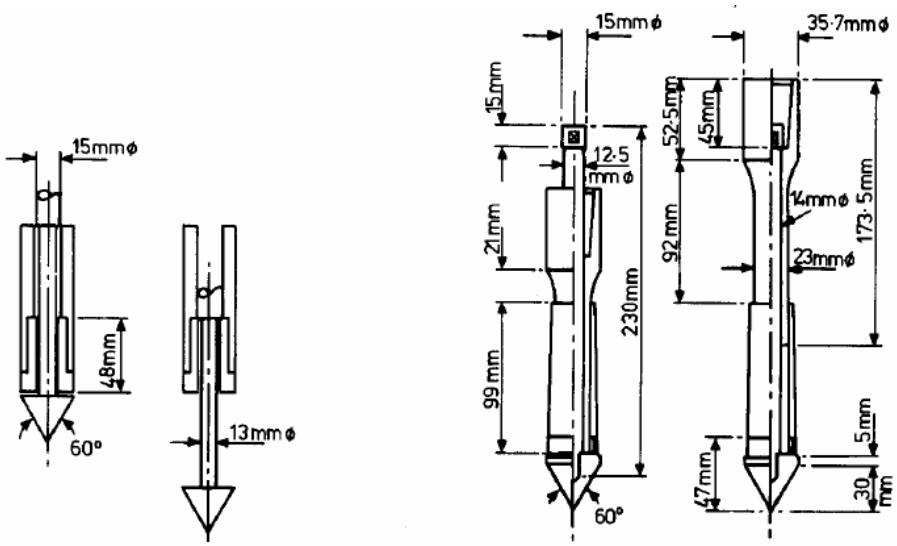

Figure 3.1 Original Dutch Cone (left) and Enhanced Delft cone (right) (Lousberg & Calembert, 1974)

3.1.1 Mechanical Cone Testing

The mean of moving a mechanical cone forward is significantly more complicated than for an electric cone because force must be measured while the constituents are advancing, in order to reduce friction. How the uncomplicated Delft one works is shown below (C.R.I. Clayton, 1995):

1. The end of cone is moved forward by driving it down by 8cm at the ground level on a string of hard 15 mm length rods, which continue inside the exterior hollow rods to the ground level from the cone.

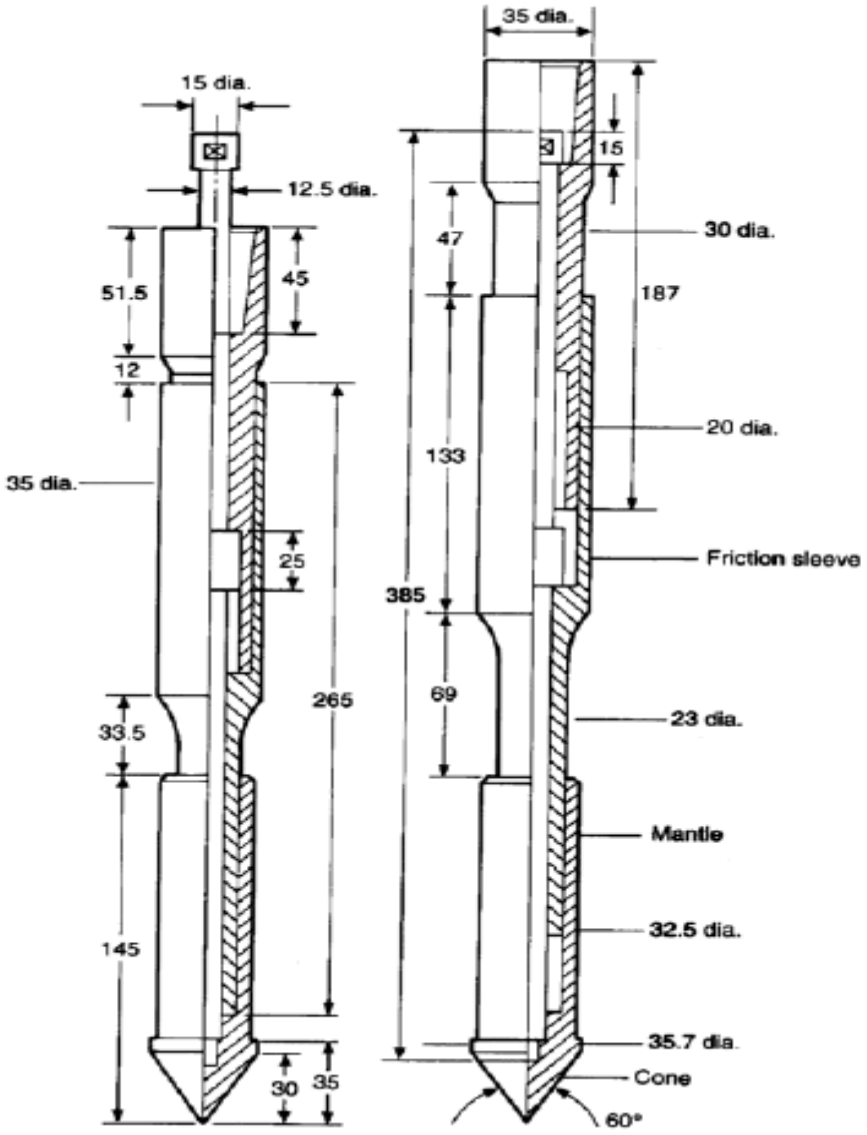

Figure 3.2 Begemann's Mechanical Friction Cone (left: wholly closed, right: fully lengthened (Meigh, 1987)

2. While the cone is advancing at the approved rate, cone resistance at the ground level is gauged through a hydraulic load cell combined to a

pressure gauge, or with an electrical transducer that is placed at the peak of the rod string at the ground level.

3. After measuring the cone resistance by pushing the cone, the exterior rods are propelled by 20cm. The cone and rods should advance together during the last 12 cm pushed.

4. Redo the whole process until you gain the intermittent force measurements at 20cm depth intervals.

5. In every meter of each measurement new outer and inner rods are added.

The proceeding evolves more complicated when the mechanical friction cone is employed, and the proceeding is shown below

1. The inner rods are pushed and the cone end by 4cm.

2. While the cone rods are moving forward, cone resistance are recorded

3. The inner rods move forward continuously and they are involved in the friction sleeve.

4. The total of the side friction and the cone resistance leading to recoding the total force.

5. By deducting the first recorded force from the second one, the force on the friction sleeve is gained.

6. In the ending step the exterior rods are moved down by 20 cm and friction sleeve with them are taken for the final 16cm and the cone for the final 12cm.

7. Redo the proceeding until a record of cone resistance and side friction every 20cm are gained.

8. In every meter new exterior and inner rods are added.

The Delft and Begemman friction cones are uneven and uncomplicated to employ and to sustain because they are mechanical. If the equipment is suitably kept and the testing is carried out with caution, dependable results are gained. However, opposite to this they have a structure of measurement which can cause serious mistakes (C.R.I. Clayton, 1995).

3.1.2 Electrical Cone Testing

With regard to cone manufacture and measuring and data logging, Electric cones are more high-priced. However, they have many benefits that it is simple to employ, it is possible to measure forces immediately their application points and it can give almost continued information as regards soil deepness. A diagrammatic picture of an electric cone is shown in Figure 3.3. Cone resistance is recorded as a guideline, and side friction measurement is significantly normal as well. The below subsequent measurements, moreover, may be used according to the cone maker (C.R.I. Clayton, 1995). .

1. cone slant, to check that the cone is not moving aimless

2. pore pressure (in the 'piezocone')

3. soil resistivity (for example employed in pollution studies);

4. ground vibration, employing three-component geophones(in the 'seismic cone ')

5. gamma-ray backscatter (to determine density);

6. pressureemeter values; and

7. sound (the 'acoustic' penetrometer).

Meigh shows the benefits of the electric penetrometer and the lists of it are included below(Meigh, 1987):

1. The outcome of the certainty and repeatability are enhanced especially in weak soils;

2. Better border of thin layers are gained (because readings can be carried out more often);

3. It operates with faster comprehensive speed.

4. There is a chance of broadening the scope of sensors in or above the tip

5. There are more easily handled data.

Because of the advantages something like speed and convenience, the electric cone is employed in a lot of countries, even though mechanical cones are still normally used. Comparing the mechanical cones with electric friction cones, different geometries will be shown in Figure 3.2 and Figure 3.3. Electric cone can be ready to gain data such as drawing of sleeve friction and cone resistance as well as to give guess of soil parameters and soil kind when the penetration is executed. This provides a chance to the engineer to decide concerning the design of a ground examination while testing continues (C.R.I. Clayton, 1995).

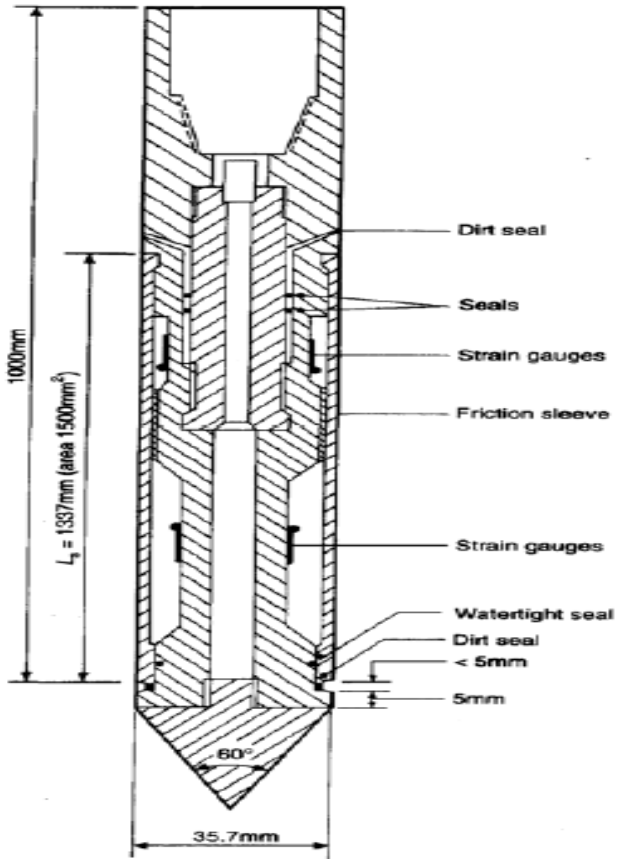

Figure 3.3 Electric Friction cone after Meigh (Meigh, 1987)

3.1.3 The Piezocone

When the cone testing is processing, the recording pore water pressure is not as usual as recording cone resistance and side friction. However, when testing soft soil layers, the awareness of the large potential of this equipment has been raised. The equipment contains a porous part with

an electronic pore pressure transducer installed in a space behind the porous part. There are 3 preferred spots for this porous part presented in below Figure 3.4 (C.R.I. Clayton, 1995).

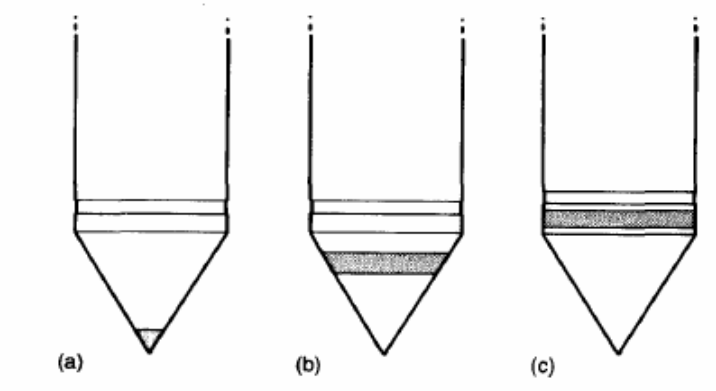

Figure 3.4 Locations of Porous Tips on Piezocones

3.1.4 The Seismic Cone

The Seismic Cone Penetration Test (SCPT) is used to determine the variation with depth of the shear (and longitudinal) wave velocity at several different sites (Karl, Haegeman, & Degrande, 2006). Seismic cones include one or two three-constituent geophone arrays installed inside and they have some distance behind the friction sleeve. The vertical breadth between the geophone arrays will be arranged about 1 m when two arrays are employed. It has been recently verified as a useful equipment to determine the standard value of very small strain stiffness (G_0) through parallel cross-hole testing or more usually down-hole testing (C.R.I. Clayton, 1995).

SCPT is arranged by employing dual cone. A cone is penetrated by using a CPT truck. Two triaxial accelerometers named 1 and 2 in the Figure 3.6 are installed in the cone's housing at an approximate distance 1m between them. The accelerometers have flat frequency response over the total frequency range of interest. Miniature geophones are normally employed. These miniature geophones have a natural frequency inside this frequency range and thus, are not adequate for a detailed record of the response. The source of seismic waves is made up of a steel beam. The steel beam is loaded by a conventional sledgehammer or a mechanical

swing hammer with alterable dropping height to produce a vertically spreading shear wave in the soil (Karl et al., 2006).

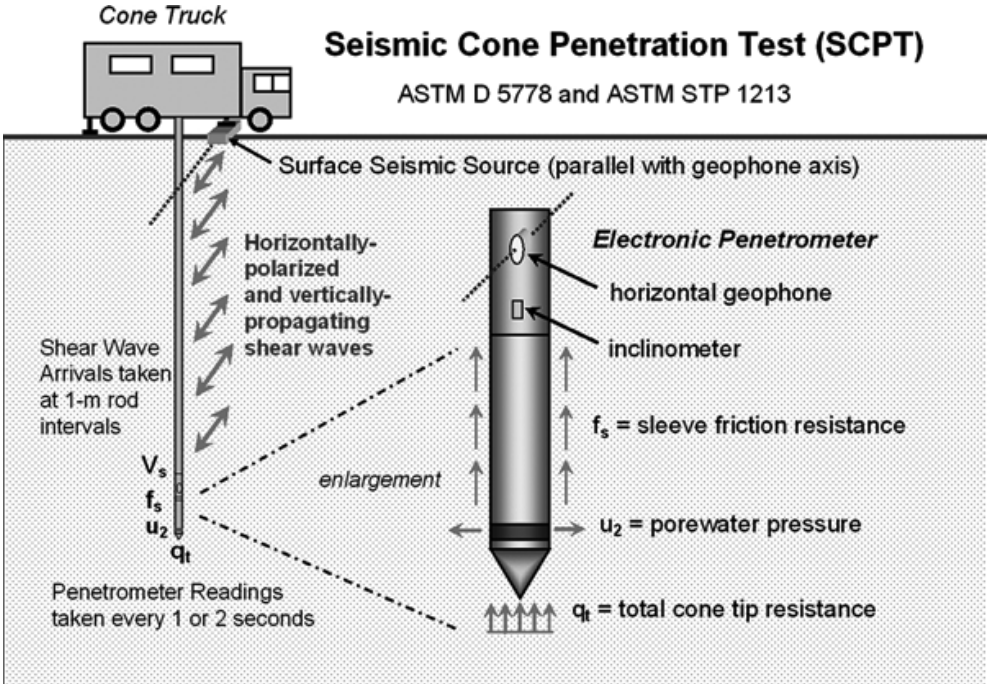

Figure 3.5 Seismic Cone Penetration Test (P. Mayne, 2007)

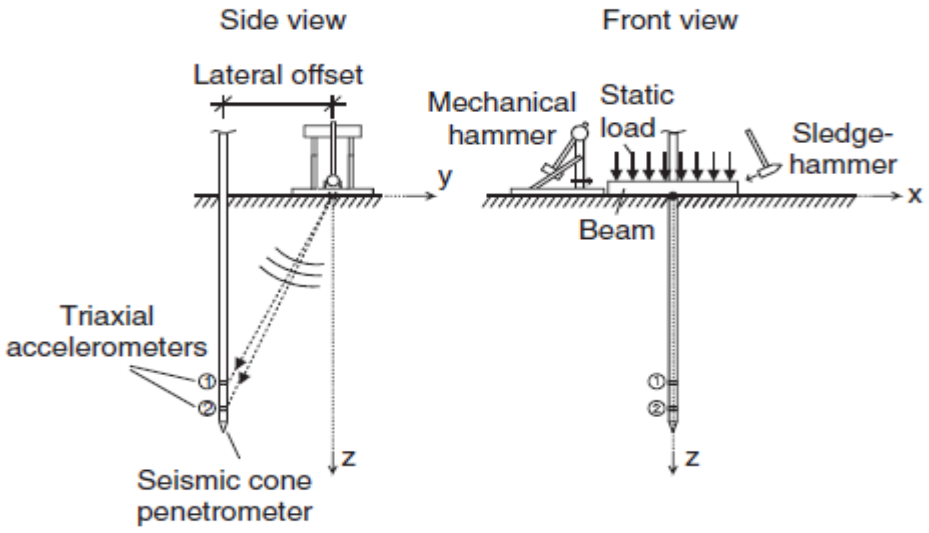

Figure 3.6 Side and front View of Seismic Cone Penetration Test (Karl et al., 2006)

3.2 Cone Penetration Test Interpretation

3.2.1 Stratigraphy

The CPT is a great equipment to profile the changes of layers. Through this test, the face between soil strata is delineated and inclusions, stringers, and small lenses are discovered under the ground. The tip, sleeve and pore-water reading from information from a CPT sounding are plotted again the depth (P. Mayne, 2007). Below Figure 3.7 indicates these values from CPTU sounding in a sand layer (in the Fraser River delta outside Vancouver, BC).

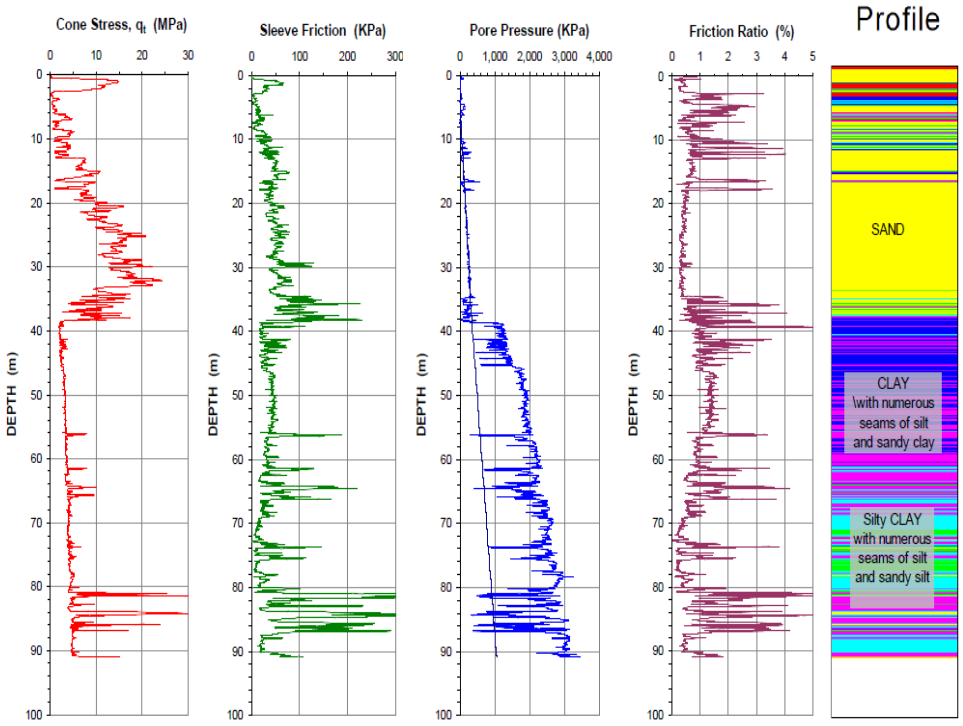

Figure 3.7 CPTU Sounding Drawing with Profiling Soils Depending on the Eslami-Fellenius (Eslami & Fellenius, 1997). Information from Amini et al. (Amini, Fellenius, Sabbagh, Naesgaard, & Buehler, 2008)

The global soil stratigraphy can be divided into four major zones as shown below. The coloured column to the right part is gained straight from soil stratigraphy employing data from CPTU.

0m	-	2.6m	coarse sand
2.6m	-	6.0m	clay, silty clay
6.0m	-	13.0m	intermediate to fine sand and silty sand (fine sand quantity = 30% to 80%)
12.5m	-	16.0m	fine sands small silt
16.0m	-	34.0m	fine to intermediate sand
34.0m	-	38.0m	silty sand
38.0m	-	70.0m	clay with many silt seams and sandy clay
From	70.0m		Silty clay with seams of silt and sandy silt

The pore pressure dispersion in the clay stratum under 38m depth is increasing and the pore pressure head above ground is around 7m, depending on the pore pressure dissipation measurements.

3.2.2 Soil Classification

There are many ways to classify soils. In here, the soil classification by Roberton is shown. Robertson and Campanella established two classification charts. The parameter (q_t) is used for the ordinate and two parameters (R_f and B_q) are used for the x-axis in Figure 3.8. q_t is the total cone resistance corrected based on the u recorded during cone penetration. α is the ratio of the shoulder area (A_n) uninfluenced by the pore water pressure divided by the total shoulder area (A_c) (P. K. Robertson, Campanella, Gillespie, & Greig, 1986).

$$q_t = q_c + u_2*(1-A_n/A_c) \qquad (A_n/A_c)=\alpha$$

$$R_f = 100*f_s/q_t$$

$$B_q = (u_2-u_o)/(q_t-\sigma_{vo})$$

In the above

B_q = the pore pressure ratio

u_2 = pore pressure measured with a porous filter located closely

back the base of the cone during penetration

u_o = hydrostatic pore pressure

q_c = cone penetration resistance

q_t = cone resistance corrected according to u value

σ_{vo} = total vertical(overburden) stress

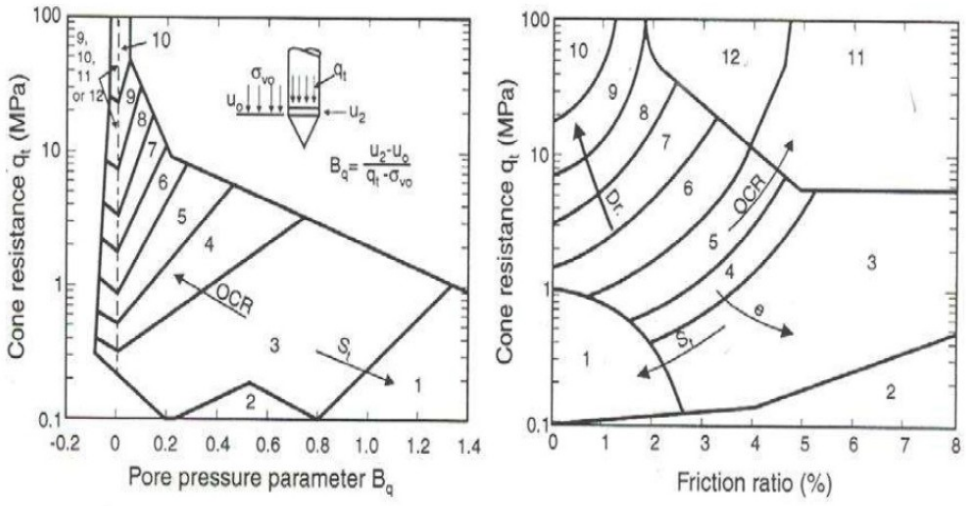

Figure 3.8 Soil Classification graphs (Robertson et al.1986)

The charts are divided into twelve zones as shown below. It could be employed to judge soil kind during and directly after the CPT_u. (P. K. Robertson et al., 1986).

1. Sensitive fine-grained soil
2. Organic soil material
3. Clay
4. Silty clay to clay
5. Clayey silt to silty clay
6. Sand silt to clayey silt
7. Silty sand to sandy silt
8. Sand to silty sand
9. Sand
10. Sand to gravelly sand
11. Very stiff fine-grained soil
12. Sand to clayey sand

There are many influential elements when both charts are employed. Employing both charts apparently causes different indications. In that situation it is needed to mention the opinion of the expertise (Meisina, 2013).

Robertson(1990) suggested a grown soil classification chart from the Robertson et at. (1986). Robertson (1990) has newly brought two parameters to consider the effect of the lithostatic pressure that may apply at significant depths (Figure 3.9) (P. Robertson, 1990) .

Q_t normalized = $(q_t-\sigma_{vo})/\sigma'_{vo}$

R_f normalized = $f_s/(q_t-\sigma_{vo})$

$B_q$normalized Bq = $\Delta U/(q_t-\sigma_{vo})$

ΔU = $U_2 - U_o$

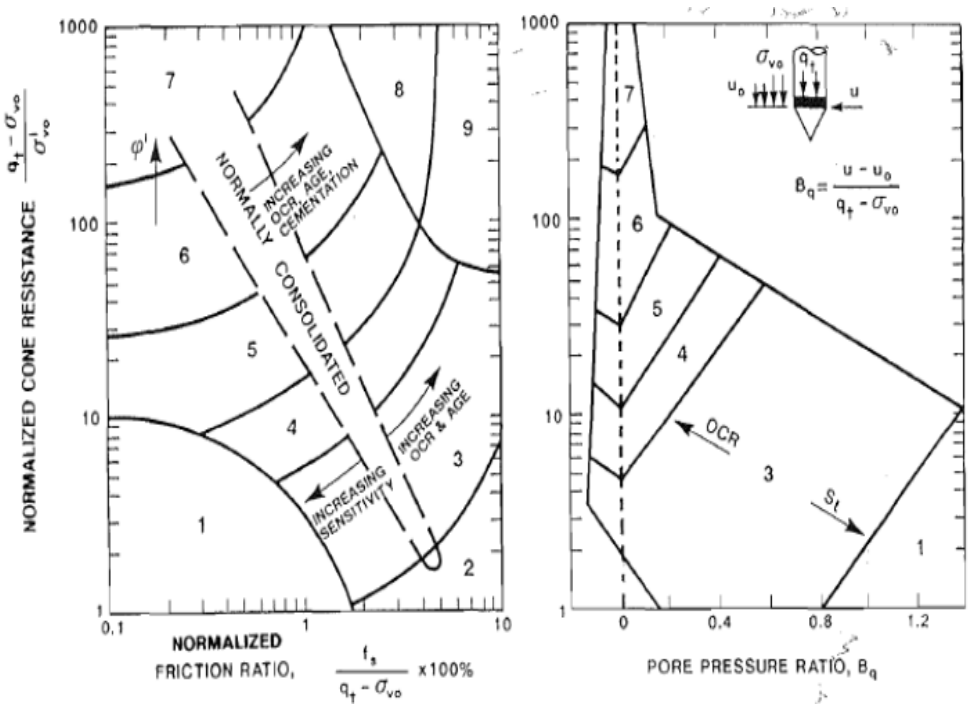

Figure 3.9 Upgraded Soil Classification Graphs (Robertson et al. 1990)

The classification zones are divided into 9 zones as shown below

1. Sensitive, fine-grained soils	2. Organic soils and peat
3. Clays – clay to silty clay	4. Silt mixtures – clayey silt to silty clay
5. Sand mixtures – silty sand to sandy silt	6. Sand – Clean sand to silty sand
7. Sand to gravelly sand	8. Sand – clayey sand to very stiff sand (Heavily oversolidated or cemented)

9. Very stiff, fine-grained (Heavily oversolidated or cemented)

The first and last two soil types are identical to those employed by Robertson at al (1986). The soil type from 3 to 7 is the same as the original one from 3 to 7. The Robertson (1990) normalized classification graphs and they have been widely employed by engineers like Robertson et al (1986). The normalization is to offset the cone stress that is affected by the overburden stress. It is recommended to employ the Figure 3.9 for depths of more than 30 m from the ground surface (B. H. Fellenius, 2014).

3.3 Application of Cone Penetration Test

A lot of early cone data was directly applied for pile design. The data gained from field experience has the merit that can create dependable outcomes when they are used in identical situations. Direct CPT methods have been recently grown for other use of liquefaction assessment and design of shallow foundations as well. The direct use of CPT has merit for granular soils where employment of relative density can create wrong results (P. K. Robertson, 1986).

3.3.1 Applications to Shallow Foundations

The CPT tip resistance is used to measure the ultimate strength of the soil. Thus, a direct connection between the q_t of CPT and foundation BC (q_{ult}) has been tried to achieve by using empirical means and/or experimental research (Sanglerat, 1972) (Frank & Magnan, 1996) (Lunne & Keaveny, 1995) (Eslami, 2006).Two means will be shown below for sands and clays.

Schmertmann shows a direct relation in sand between q_t and q_{ult} as represent in Figure 3.10 when the below situations related to the foundation size (B) and penetrated foundation depth (z_e) are satisfied (J. H. Schmertmann, 1978):

When $B > 0.9m$ (3ft), embedment $z_e \geq 1.2m$ (4ft).

When $B \leq 0.9m$ (3ft), embedment $z_e \geq 0.45m + 0.5*B$

When the cone tip resistance is between $20 \leq q_t \leq 160$ tsf, the ultimate BC stresses can be roughly by:

Square footings: $q_{ult} = 0.55*\sigma_{atm}*(q_t/\sigma_{atm})^{0.785}$

Strip footings: $q_{ult} = 0.36*\sigma_{atm}*(q_t/\sigma_{atm})^{0.785}$

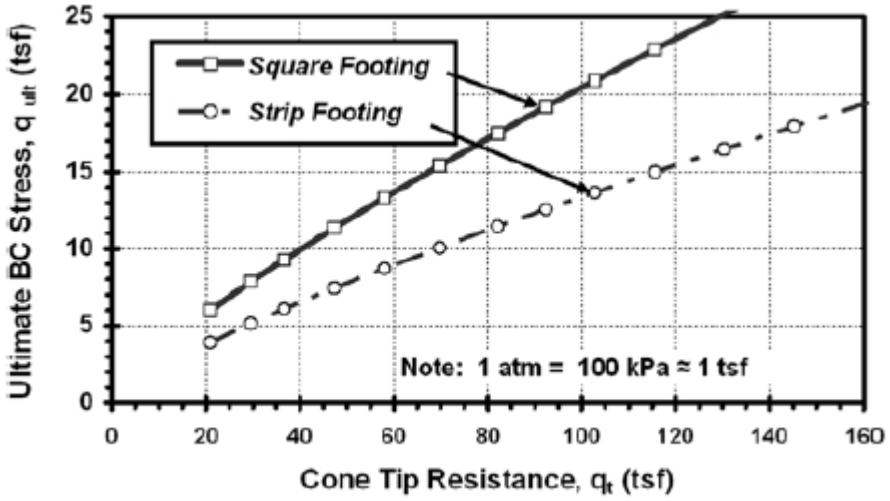

Figure 3.10 Relation between q_t and q_{ult} in Sands (J. H. Schmertmann, 1978)

Above σ_{atm} = reference stress is identical to one atmosphere (1atm =100kPa ≒ 1tsf).

Tand et al. gave a definition of a parameter R_k below for shallow footing on clays (Tand, Funegard, & Briaud, 1986):

$R_k = (q_{ult} - \sigma_{vo})/(q_t - \sigma_{vo})$

Above equation is gained through Figure 3.11. The R_k value is changed according to the embedment ratio (H_e/B). H_e = penetrated depth and B = foundation breadth. In the Figure 3.11 the undamaged clay represents upper curve and the cracked clay represents lower curve.

By reorganizing above mentioned equation, the BC for shallow foundations on clay is represented below:

$q_{ult} = \sigma_{vo} + R_k*(q_t - \sigma_{vo})$

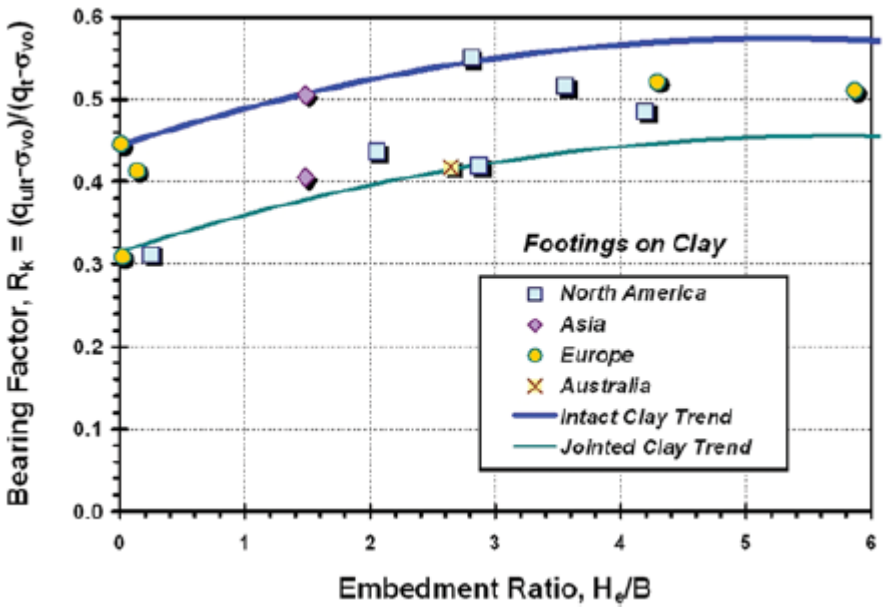

Figure 3.11 Applied CPT Means to Determine Ultimate Bearing Capacity (Tand et al., 1986)

3.3.2 Applications to Pilings and Deep Foundations

The static cone penetrometer is very similar to a pile. The shaft resistance is similar form of the sleeve friction recorded close to the higher position of the cone. The toe resistance is similar to the form of the directly applied and recorded cone stress. Although they are similar, there is no scientific evidence why cone stress and sleeve friction recorded would interact with the continuing static resistance of a pile. However,

the static cone results lead to ambiguous design if they do not have specific site interaction. CPT has been used to know pile capacity since it grew in the Netherlands. In order to determine pile capacity, seven means that are shown below have been developed. Six means are based on the mechanical or the electric cones and other one is based on the CPTU. CPTU-based method is the Eslami-Fellenius method and this method can be employed to CPT results. This last method is introduced in this part (B. H. Fellenius, 2014).

1. Schmertmann and Nottigham

2. deRuiter and Beringer (usually named as the Dutch Method or the European Method)

3. Bustammante and Gianselli (usually named as the LCPC Method or the French Method)

4. Meyerhof (method for sand)

5. Tumay and Fakhroo (method used only to piles in soft clay)

6. The ICP method

7. Eslami and Fellenius

The Eslami-Fellenius employ CPTU and this tool has a gage to record the pore pressure at the cone (normally very near above the cone and at the cone shoulder that is called U_2 position), which significantly advance on the static cone. By using the piezocone, CPTU, the more reliable soil parameters can be related to the cone data and a more careful examination is carried out in detail for soil parameters (B. H. Fellenius, 2014).

Toe Resistance

The cone stress is changed to obvious "effective cone stress", q_E and the effective cone stress is gained by deducting the recorded pore pressure ,U_2, from the recorded whole cone stress (corrected for pore pressure working opposite to the shoulder) in the Eslami and Fellenius CPTU mean ((Eslami, 1996) (Eslami & Fellenius, 1995) (Eslami & Fellenius, 1996) (Eslami & Fellenius, 1997) (B. Fellenius & Eslami, 2000). The pile unit toe resistance represents the geometric average of the effective cone stress covering influence zone that relies on the soil

stratum and the geometric average eliminate potentially unsuitable effects of specially unselected "peaks and troughs", which the uncomplicated arithmetic average employed for the CPT means does not remove. When a pile is set up through a weak soil into a dense soil, the mean is gained covering an influence zone affecting between 4b under the pile toe and a height of 8b over the pile toe. When a pile is reversely set up through a dense soil into a weak soil, the mean above the pile toe is decided covering an influence zone, height of 2b, upper the pile toe. The equation about this relationship is shown below (B. H. Fellenius, 2014).

$r_t = C_t * q_{Eg}$

Above r_t =pile unit toe resistance, C_t= toe correlation coefficient (toe adjustment factor) –same as unity in most cases, q_{Eg}= geometric mean of the cone stress covering the influence zone following correction for pore pressure on shoulder and change to "effective" stress

The toe correlation coefficient, C_t, named toe adjustment factor as well, is changed according to the pile size (toe diameter). When the pile diameter is large, the large movement is needed to mobilize the toe resistance. Thus, the "usable" pile toe resistance reduces when the pile toe diameter increases. The adjustment factor should be decided for pile diameters that are larger than around 0.4m depending on the relation below (B. H. Fellenius, 2014).

C_t =1/3b (b is meter), C_t = 12/b (b is inches), C_t = 1/b (b is feet)

where, b= pile diameter

Shaft Resistance

The pile unit shaft resistance is related to the mean "effective" cone stress as well with an adjustment in accordance with soil kind. The C_s, correlation coefficient, is employed in cone stress and sleeve friction. The sleeve friction value, however, is used indirectly because the sleeve friction is a more changeable value than the cone stress. The equation to gain pile unit shaft resistance is shown below(B. H. Fellenius, 2014).

$r_s = C_s * q_E$

Above r_s = pile unit shaft resistance, C_s= shaft correlation coefficient that is changed depending on the soil kind gained from the Eslami - Fellenius soil profiling in Figure 3.12 and Table 3.1, $q_E = q_t - u_2$.

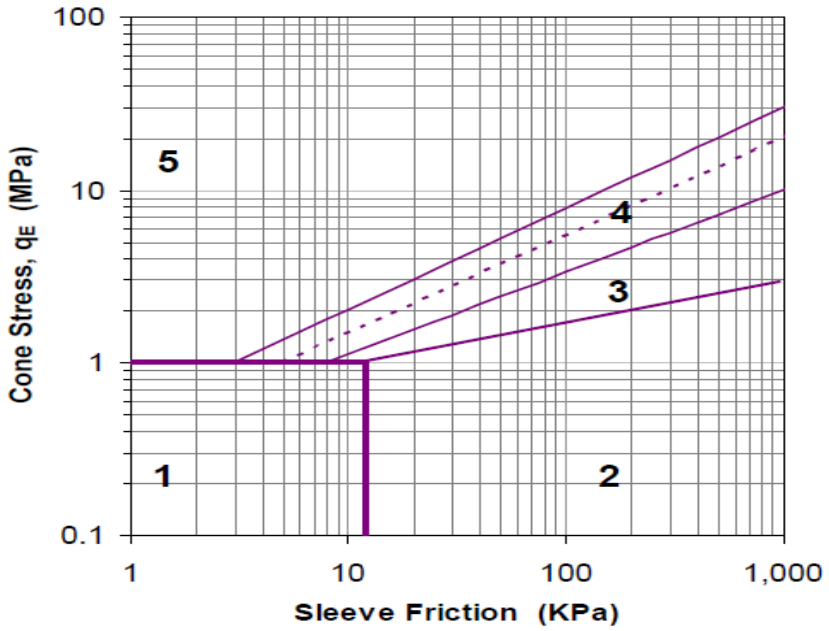

Figure 3.12 The Profiling Chart (Eslami, 1996) (Eslami & Fellenius, 1997) (1. Very soft clay, or sensitive soils 2. Clay or Silts 3 Clayey silt or silty clay 4a. Sandy silt 4b. Silty sand 5. Sand to sandy gravel)

Table 3.1 Coefficient, C_s

Soil Type	C_s
1. Soft sensitive soils	8.0%
2. Clay	5.0%
3. Silty clay, stiff clay and silt	2.5%
4a. Sandy silt and silt	1.5%
4b. Fine sand or silty snad	1.0%
5. Sand to sandy gravel	0.4%

3.3.3 Application to Liquefaction Resistance

One of the main advantages of the CPT is that a continued profile of penetration resistance can be gained. The continuous profile helps to gain detailed information of the soil strata and the stratigraphy from the CPT is useful to grow liquefaction-resistance profiles. However, CPT-based interpretation must be checked with standard penetration test in order to confirm soil types and liquefaction-resistance interpretation (Youd et al., 2001).

The CPT Clean Sand Base Curve offered by Robertson and Wride to straight determine CRR for clean sands (FC≤ 5%) from CPT data in Figure 3.13 (P. Robertson & Wride, 1998). The Figure 3.13 was improved from past CPT-recorded data amassed from some investigations and data by Stark and Olson and Suzuki et al. are contained as well (Stark & Olson, 1995; Suzuki, Tokimatsu, Koyamada, Taya, & Kubota, 1995). The Figure 3.13 is accepted with magnitude 7.5 earthquakes. The Figure 3.13 represents computed cyclic resistance ratio (CRR) drawn depending on the corrected, dimensionless and normalized CPT resistance q_{c1N} from locations where surface effect of liquefaction were or were not detected after previous earthquakes. The CRR bending line divides the liquefaction zone from non-liquefaction zone (Youd et al., 2001). Through the Figure 3.13, we can guess if a site will have liquefaction.

The normalization of end resistance employing below equation is needed for the CPT procedure. This change produces dimensionless and normalized cone penetration resistance q_{c1N} (Youd et al., 2001).

$q_{c1N} = C_Q * (q_c/P_a)$ where, $C_Q = (P_a/\sigma'_{vo})^n$

From the above C_Q = normalization factor for cone penetration resistance. P_a = 1 atm (=100kPa = 1tsf) and is identical unit to that of the σ'_{vo}. n = exponent that changes according to the soil type. q_c = field cone penetration resistance at the tip. C_Q has large values due to low overburden pressure at shallow depths. However, values larger than 1.7 should not be adopted. n value is ranged from 0.5 to 1.0 with the grain characteristics of the soil (Olsen, 1997).

The clean-sand base curve in the Figure 3.13 is roughly represented by below equation (P. Robertson & Wride, 1998):

If $(q_{c1N})_{cs} < 50$ $CRR_{7.5} = 0.833*[(q_{c1N})_{cs}/1000] + 0.05$

If $50 < (q_{c1N})_{cs} < 160$ $CRR_{7.5} = 93*[(q_{c1N})_{cs}/1000]^3 + 0.08$

From the above $(q_{c1N})_{cs}$ =clean-sand cone penetration resistance normalized to roughly 100kPa (1atm).

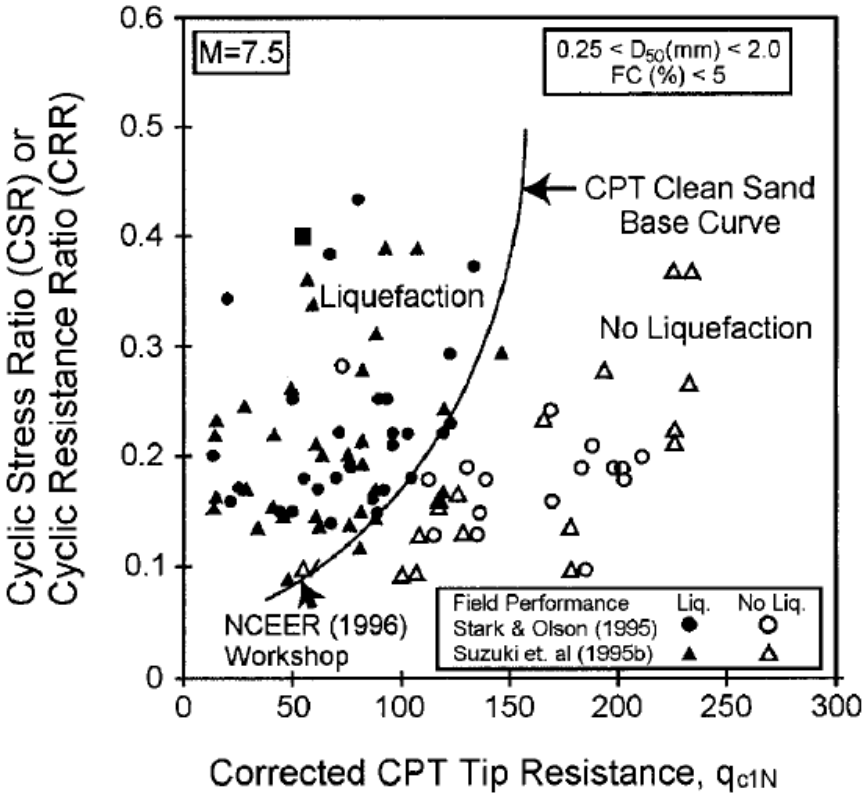

Figure 3.13 The Graph to Compute CRR from CPT Data from Gained Case History (P. Robertson & Wride, 1998)

Juang and Jiang showed the chart in the Figure 3.14 in order to express the liquefaction resistance. This chart represents the probability of liquefaction P_L and the scope of P_L value is from 0.1 to 0.9. The curve is mathematically represented in the below equations (Juang, Chen, Jiang, & Andrus, 2000).

$CRR_{PL=0.1} = 0.025*(e^{0.14qc1})$

$CRR_{PL=0.2} = 0.033*(e^{0.14qc1})$

$CRR_{PL=0.3} = 0.038*(e^{0.14qc1})$

$CRR_{PL=0.5} = 0.046*(e^{0.14qc1})$

$CRR_{PL=0.7} = 0.057*(e^{0.14qc1})$

$CRR_{PL=0.9} = 0.085*(e^{0.14qc1})$

Above, CRR= Cyclic Resistance Ratio, P_L = probability of liquefaction and q_{c1} = Normalized Cone stress

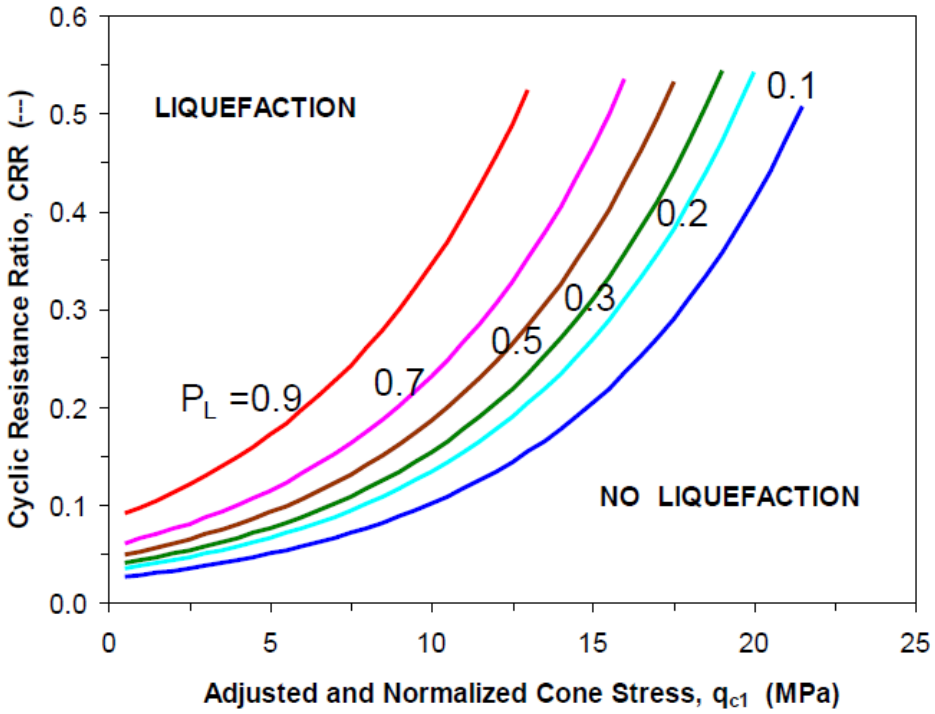

Figure 3.14 Relation CRR and q_{C1} according to the P_L (Juang et al., 2000)

3.4 Estimated Parameters from CPT

A lot of geotechnical parameters are widely spread. Their reliability relies on the experience of the user who has applied parameters. The most

important thing is the experience of the user when the parameters are used through the correlations. No formula between the CPT test results and geotechnical parameters should be applied without considering the correlations that are gained from different tests outcomes at the site (B. H. Fellenius, 2014).

3.4.1 Undrained Shear Strength

CPT results are employed to gain undrained shear strength. It is popular to apply CPT results to gain undrained shear strength although a lot of means such as unconfined compression test, triaxial testing, in-situ vane, direct shear, simple shear, standard penetration test, etc. are used to obtain undrained shear strength. Below equation is normally used to obtain the undrained shear strength form CPTu (Kulhawy & Mayne, 1990).

$$\tau_u = (q_t - \sigma_v)/N_{kt}$$

From the above τ_u= undrained shear strength, q_t = cone stress corrected for pore water pressure on shoulder [$=q_c+u_2(1-\alpha)$], σ_v = entire overburden stress, N_{kt} = a coefficient.

N_{kt} is in range below and the values are normally used. However, the use of CPT value in fissured clays is restrained (Meisina, 2013).

Soft clay: $N_{kt} = 14\pm4$

Overconsolidated clay: $N_{kt} = 17\pm5$

Fissured clay: $N_{kt} = 10\pm30$

3.4.2 Friction Angle, phi

The CPTu test results are employed to gain effective friction angle of sand by using below equations (B. H. Fellenius, 2014).

$$tg\varphi' = C_\varphi * \log(q_t/\sigma'_v) + K_\varphi$$

From above φ' = effective friction angle, C_φ = a coefficient; $C_\varphi \fallingdotseq 0.37(=1/2.68)$, K_φ = a coefficient; $K_\varphi \fallingdotseq 0.1$, q_t = cone stress corrected for

pore water pressure on shoulder [$=q_c+u_2(1-\alpha)$], σ'_v = effective overburden stress.

3.4.3 Overconsolidation Ratio, OCR

The correlation between the CPT_u test results and the overconsolidation ratio, OCR has been introduced and the equation is shown below (Kulhawy & Mayne, 1990).

$$OCR = C_{OCR}*(q_t-\sigma_v)/\sigma'_v$$

From above OCR=overconsolidation ratio, C_{OCR} = a coefficient ($0.2<C_{OCR}<0.3$), q_t= cone stress corrected for pore water pressure on shoulder [$=q_c+u_2(1-\alpha)$], σ_v= entire overburden stress, σ'_v= effective overburden stress.

3.4.4 Earth Stress Coefficient, K_o

Earth stress coefficient, K_o, is related to the CPT_u results and the equation is shown below about this (Kulhawy & Mayne, 1990).

$$K_o = C_K*(q_t-\sigma_v)/\sigma'_v$$

From above, K_o = earth stress coefficient, C_K = a coefficient($\fallingdotseq 0.1$), q_t= cone stress corrected for pore water pressure on shoulder [$=q_c+u_2(1-\alpha)$], σ_v= total vertical stress, σ'_v = effective overburden stress.

3.4.5 Sensitivity

The sensitivity (S_t) is regarded as a standard to judge a hard field performance and problematic construction in silts and soft clays. The friction sleeve value obtained from the CPT can be indicated for remolded undrained shear strength: $f_s \fallingdotseq S_{ur}$ (Gorman, Drnevich, & Hopkins, 1975). The index of the sensitivity(S_t) from soil layers may be gained by representing the proportion of top shear strength to changed value (P. Mayne, 2007).

$$S_t \fallingdotseq 0.073*(q_t-\sigma_{vo})/f_s$$

From above S_t = sensitivity, σ_{vo} = total vertical stress, f_s = cone sleeve friction, q_t= cone stress corrected for pore water pressure on shoulder [$=q_c+u_2(1-\alpha)$].

3.4.6 Relative Density

It is normal to calculate relative density (D_r) by in-situ tests in clean sands that have fines content less than 15%. Jamiolkowski et al. recently re-examined a lot of calibration chamber tests (CCT) data and he discovered a relation between normalized cone tip stress and relative density. The relation is shown below and the influence of sand compressibility is represented in Figure 3.15(Jamiolkowski, Lo Presti, & Manassero, 2001). The Figure 3.15 shows that the higher compressibility the soils have, the higher D_r values are gained when the normalized tip resistance is same.

$$D_r = 100*[0.268*[\ln(q_t/\sigma_{atm}) - \ln(\sigma'_{vo}/\sigma_{atm})^{0.5}]-0.675]$$

From above D_r = relative density of sand, q_t = cone stress corrected for pore water pressure on shoulder [$=q_c+u_2(1-\alpha)$], σ_{atm}=atmospheric pressure (1 atm = 1 bar = 100kPa ≒1tsf ≒14.7 psi).

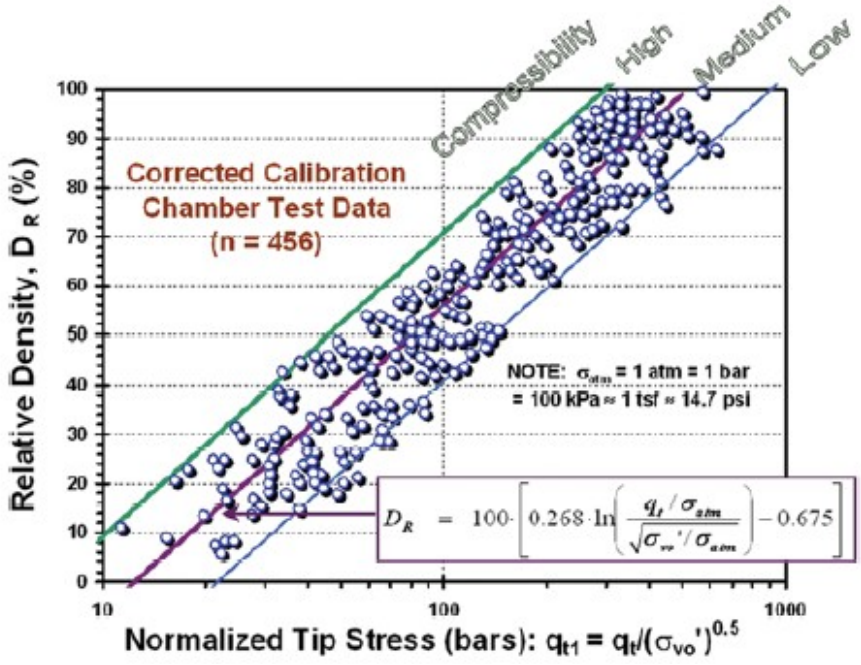

Figure 3.15 Relationship among Relative Density, Normalized Tip Stress and Sand Compression. (Jamiolkowski et al., 2001)

3.4.7 Constrained Modulus

The relation between cone penetration resistance (q_c) and constrained modulus (M) is shown below.

$M = 1/m_v = \alpha * q_c$

From above m_v = volumetric compressibility = $\Delta v/v/\Delta p$. α value is changed according to the cohesive soil types and cone resistance values shown below Table 3.2. However, α value is normally ranged from 1.5 to 4.0 for sand (P. K. Robertson & Campanella, 1983).

Table 3.2 Estimation of Constrained Modulus, M (Mitchell & Gardner, 1975)

$q_c < 0.7$MPa	$3 < \alpha < 8$	Clay with low plasticity (CL)
0.7MPa $< q_c <$ 2.0MPa	$2 < \alpha < 5$	
$q_c >$ 2.0MPa	$1 < \alpha < 2.5$	
$q_c >$ 2.0MPa	$3 < \alpha < 6$	Silts with low plasticity (ML)
$q_c <$ 2.0MPa	$1 < \alpha < 3$	
$q_c <$ 2.0MPa	$2 < \alpha < 6$	Highly plastic silts and clays (MH, CH)
$q_c <$ 1.2MPa	$2 < \alpha < 8$	Organic silts (OL)
$q_c <$ 0.7MPa		Peat and organic clay (P_t, OH)
$50 < w < 100$	$1.5 < \alpha < 4$	
$100 < w < 200$	$1 < \alpha < 1.5$	
$200 > w$	$0.4 < \alpha < 1$	

note: w=water content

3.4.8 Shear Wave Velocity

Shear wave velocity (V_s) is normally gained in every material such as gravels, fractured and intact rocks, gravels, sands, silts and clays. Shear wave velocity is obtained by using laboratory tests and various field geophysical tests (Campanella, 1994). Using SCPT and downhole geophysics test is the best way to gain shear wave velocity. However, if SCPT is not applicable, it may be needed to gain shear wave velocity through empirical connections and the empirical connection also helps to verify the gained shear wave velocity (Lunne, Robertson, & Powell, 1997) (Schnaid, 2005). The correlation between V_s and cone penetration test is represented below according to the soil types.

Sands: $V_s = 277*(q_t)^{0.13} *(\sigma'_{vo})^{0.27}$ (Baldi, Bellotti, Ghionna, Jamiolkowski, & Lo Presti, 1991)

Clays: $V_s = 1.75*(q_t)^{0.627}$ (P. W. Mayne & Rix, 1995)

From above V_s = shear wave velocity, q_t = stress corrected for pore water pressure on shoulder [$=q_c+u_2(1-\alpha)$], σ'_{vo} = effective overburden stress (MPa).

3.4.9 Soil Unit Weight

Soil unit weight (γ) is usually gained by bringing undisturbed samples from under the ground and checking a weight of the soil volume. When this method is not available, the soil unit weight is estimated below correlations and in the Figure 3.16(P. Robertson, 2010a).

$$\gamma/\gamma_w = 0.27(\log R_f) + 0.36[\log(q_t/P_a)] + 1.236$$

From above R_f =friction ratio [$= (f_s/q_t)*100$], γ_w = unit weight of water identical to unit of γ, P_a = atmospheric pressure identical to unit of q_t.

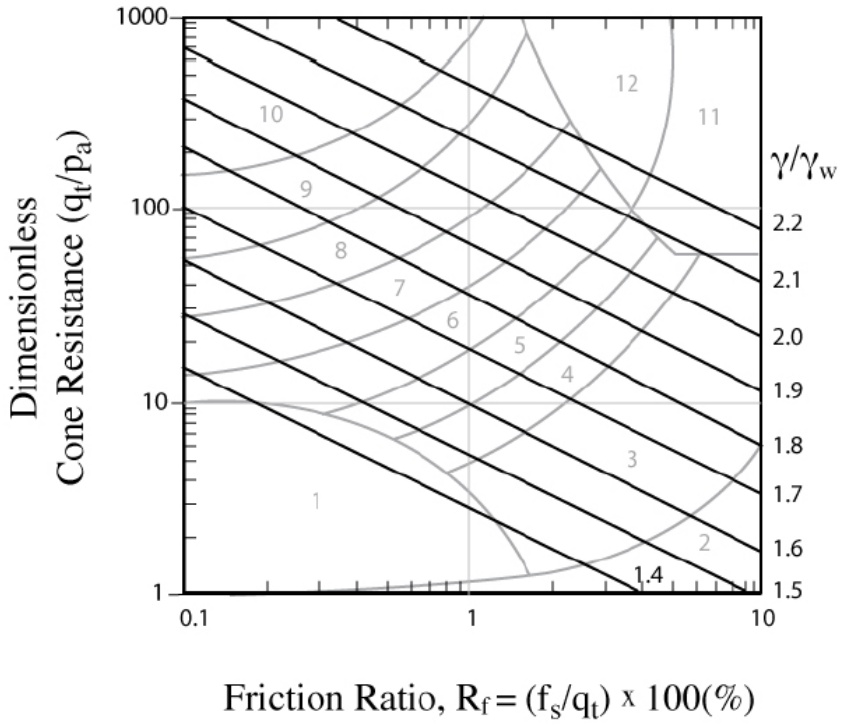

Figure 3.16 Relation between CPT and γ/γ_w

3.4.10 Hydraulic Conductivity and Fine Contents

Hydraulic conductivity (coefficient of permeability) k is gained through the CPT SBT Table 3.3. The Table 3.3 gives approximate values of k. The values in the Table 3.3 are approximate but it can be used for guideline of possibility permeability (P. Robertson, 2010a)..

Table 3.3 Hydraulic conductivity (k) depending on the SBT chart (P. Robertson, 2010a).

SBT zone	SBT	Range of k (m/s)	SBT I_c
1	Sensitive fine-grained	$3x10^{-10}$to $3x10^{-8}$	N/A
2	Clay-organic soils	$1x10^{-10}$to$1x10^{-8}$	$I_c > 3.60$

3	Clay	$1x10^{-10}$to$1x10^{-9}$	$2.95 < I_c < 3.60$
4	Silts mixtures	$3x10^{-9}$to $1x10^{-7}$	$2.60 < I_c < 2.95$
5	Sand mixture	$1x10^{-7}$to$1x10^{-5}$	$2.05 < I_c < 2.60$
6	Sand	$1x10^{-5}$to$1x10^{-3}$	$1.31 < I_c < 2.05$
7	Dense sand to gravelly sand	$1x10^{-3}$to1	$I_c < 1.31$
8	*Stiff sand to clayey sand	$1x10^{-8}$to$1x10^{-3}$	N/A
9	*Stiff fine-grained	$1x10^{-9}$to$1x10^{-7}$	N/A

*Overconsolidated or cemented

In the Figure 3.17 the normalized cone parameter Q_t and F_r are connected to the Soil Behaviour Type index I_c. I_c is the radius of the concentric circles that shows the borders between SBT zones and it is effectively used to the mixed soil area (P. Robertson, 2010b). The equation about these parameters is represented below (P. Robertson, 1990).

$$I_c = ((3.47-\log Q_t)^2+(\log F_r+1.22)^2)^{0.5}$$

From above Q_t = normalized cone penetration resistance[$=(q_t-\sigma_{vo})/\sigma'_{vo}$], F_r = normalized friction ratio[$=f_s/(q_t-\sigma_{vo})$]*100%, I_c = Soil Behaviour Type index.

I_c value is used to calculate fine contents (FC) as well and the correlations between them is represented below.

$I_c < 1.26$, FC(%)=0

$1.26 < I_c < 3.5$, $FC(\%) = 1.75*I_c^{3.25}-3.75$

$I_c > 3.5$, FC(%) = 100%.

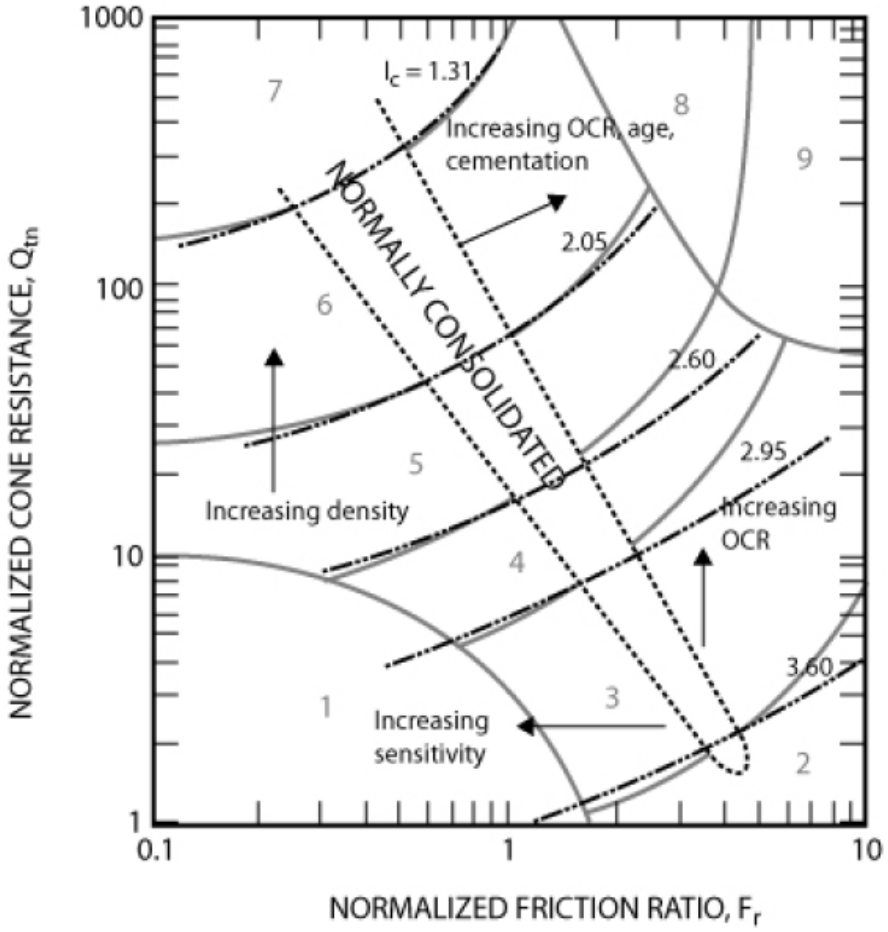

Figure 3.17 Normalized Soil Behaviour Type Chart (P. Robertson, 1990)

4 SPT-CPT Correlation

4.1 Introduction of SPT-CPT Correlation

The Standard Penetration Test (SPT) is widely employed in-situ test. Even though there have been continuous attempts to standardize the SPT process, it is still hard to have the reliability and repeatability of the SPT. A significant experience related to the design methods from the local SPT correlation has been built. However, with time passed, direct CPT design interactions will be grown as well on the basis of local experience and field examination. Therefore, it is necessary to make correlation between SPT and CPT in order to use SPT-based data that already exist(P. Robertson et al., 1983).

4.2 The Correlation between q_c and N

There have been a lot of researches (Figure 4.1) in order to express the relation between SPT N and CPT cone penetration resistance q_c as a number. The ratios of q_c/N have broad ranges and the ratios were released causing plenty of confusions. The change in released q_c/N ratio can be theoretically explained to some extent reconsidering between q_c/N ratios and mean grain size (D_{50}) as represented in Figure 4.1. It is obvious that the values of q_c/N ratios rise with rising mean grain size.

The spread data is also increasing with increasing mean grain size. This is because the embedment of gravelly sand ($D_{50} \doteqdot 1.0$mm) is significantly affected by the larger each gravel sized particles and changes of the travelled energy in the SPT data. Moreover, sands are normally stratified and heterogeneous leading to very quick change of the cone penetration resistance in CPT (P. Robertson et al., 1983). Studies by Martines and Furtado and Douglas have presented that SPT hammer type and soil density make q_c/N values changed. Particularly SPT hammer type considerably affects the q_c/N value because it has influence on the travelling energy to the rods. Data shown in the Figure 4.1 was gained by employing the standard donut type hammer with a rope and cathead system(Martins, 1963) (Douglas, 1982). It is represented by Schmertmann that q_c/N rises in sensitive clays (J. Schmertmann, 1976).

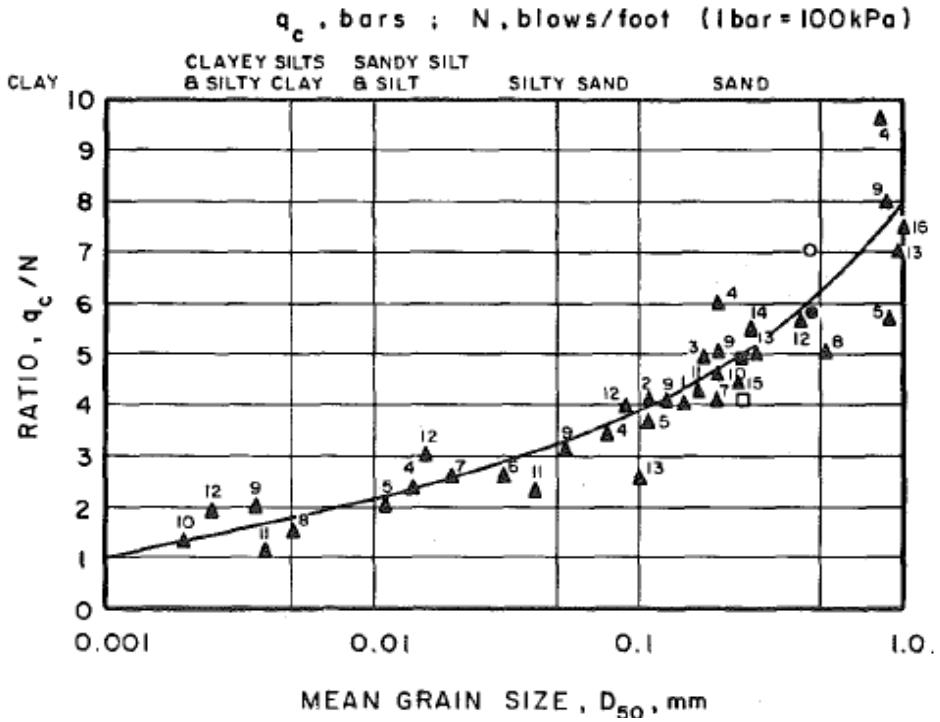

Figure 4.1 The Relation between q_c/N and Mean Grain Size from the Previous Studies

In the above Figure 4.1

1. Meyerhof(1956), 2. Meigh and Nixon 3. Rodin (1981), 4. De Alencar Velloso(1959), 5. Schmertmann(1970), 6. Sutherland(1974), 7. Thorn-

burn & Macvicar (1974), 8. Campanella et al. (1979), 9. Nixon(1982), 10. Kruizinga(1982), 11. Douglas(1982), 12. Muromachi & Kobayashi (1982), 13. Goel(1982), 14. Ishihara & Koga(1981), 15. Laing(1983), 16. Mitchell (1983).

TILBURY ISLAND SITE: □ SPT N, ER_i= 47% and ■ SPT N_c, ER_i =55%

UBC SITE, McDonald's Form: ○ SPT N, ER_i =65% and ● SPT N_c, ER_i =55%

4.2.1 Tilbury Island in Canada

The area of Tilbury Island is made up of a dense deltaic fine sand layer below around 7m depth and the mean grain size (D_{50}) of sand layer was around 0.25mm. The sand was covered by approximate 7m of a soft inter-bedded silt, clay and sand layer. Ground water level was placed approximate 1.5m from ground level. SPT was carried out employing various operators and rotary drillrigs (Longyear 34, 38 and Mayhew 100). Standard donut and safety hammers were employed respectively. The hammers had influence on anvils fixed to a string of Aw drill rods and standard 2 in. type with split liners employed as the spoons. Turning rope around the cathead two times were applied to make hammers worked. Drilling mud and casing were employed to make the Longyear drillholes drilled. The casing moved 6 m back before each SPT worked. Holes made by Mayhew 1000 and the holes are held up by bentonite mud (P. Robertson et al., 1983).

Various N values were detected by employing dissimilar hammer types and operators. The average energy was 47% of the theoretical maximum energy when the donut hammer was employed for sand. The average value of q_c/N ratios for sands was 4.2 as shown in Figure 4.1(P. Robertson et al., 1983). The N values for donut hammer were corrected to the N values of 55% energy ratio. The correction was performed presuming that N value varied with energy (J. H. Schmertmann & Palacios, 1979). After N value was corrected, q_c/N_c was 4.9. From above it is proved that the q_c/N value is 4.2 before it is corrected and this value is placed slightly low under the curve. However, when the N value is cor-

rected, q_c/N_c ratio is remarkably matched well with the historical data shown in Figure 4.1(P. Robertson et al., 1983).

4.2.2 UBC Research Site in Canada

Both SPT and CPT data were gained from the UBC research site and this is placed 8 km west of the Tilbury Island site. Upper 2 m under the ground level at the spot is made up of soft, compressible clays and silts. A sand layer is located between 2m and 13m from the ground surface. The sand consists of medium to coarse grain size (D_{50} = 0.45mm) with narrow strata of medium to fine sand. Groundwater level is around 1 m below ground level. N values are gained employing a BBS-37A rotary drillrig offered and performed by the B.C. Ministry of Highways and Transportation. Turing the rope one time around the cathead was employed to perform the standard safety hammer. By employing mud and casing, the hole was made(P. Robertson et al., 1983).

However, the SPT calibrator was unavailable at that time so that energy measurement was not performed. Both this operator and rig will be adjusted later (P. Robertson et al., 1983). In the meantime, the study by Kovacs and Salomone would show that turning the rope one time around the cathead and employing a safety hammer creates a 20% larger energy than turning the rope two times around the cathead. Thus, the amount of energy can be presumed to be around 65%-70% (W. D. Kovacs & Salomone, 1982). The mean q_c/N ratio for the sand (D_{50} =0.45mm) was 7 as indicated in Figure 4.1. If the amount of energy is corrected to 55%, q_c/N value becomes 5.7 as represented in Figure 4.1. When the level of energy is high employing one turn of the rope around the cathead, q_c/N values become higher than the historical mean (P. Robertson et al., 1983).

4.2.3 Fraser River Delta Area in Canada

The site is called as the Jacombs Road site as well and is made up of 4.5m organic sandy silts covering over approximate 15m of medium to medium-fine sands. The mean level of energy for the SPT was 56% and a mean value of q_c/N in the sand (mean D_{50}=0.23mm) is 4.4. Even if the level of energy is corrected to 55%, the mean q_c/N value is not considerably changed. q_c/N is 4.4 and D_{50} has 0.23mm. The corresponding value to these values is placed a little under the curve in Figure 4.1.

This value matches well with the historical data in the Figure 4.1(P. Robertson et al., 1983).

4.2.4 Kuwait

Windblown deposits in Kuwait are made up of fine calcareous sands. The fine calcareous sands become thicker with increasing depth and are altered to silty sands. Five spots (Andalus, Riggae, Yarmouk, Cordoba and Salmiya) were picked within the narrow area for in-situ cone tests and borings. One hollow stem auger boring and a minimum of three cone penetration tests at each spot in the area around the boring were carried out(Ismael & Jeragh, 1986).

Dutch cone penetrometer conversion equipment was used for test and the conversion equipment is changed to the CME 750-XL drill rig that are used to a mechanical cone penetrometer operator with ease. The drill has at least pulling down force of 4.54Mg (5 tons) and this force can be raised when the drill is anchored to a string of augers that are moved into the underground soils. The conversion kit is made up of a 9.98Mg (11ton) hydraulic load cell and gauges, a depth pointer instrument, pulling equipment, rod extensions, sounding tube, mantle cones and friction jacket cones. The gradually happening sounding procedure over time was followed to carry out the tests by employing friction jacket cone(Ismael & Jeragh, 1986).

The procedure is made up of determining cone point resistance for the first 3.5 cm of stroke. Afterwards the cone is involved in the friction jacket. During the final 3.5cm stroke, the cone point resistance and jacket frictional resistance are connected. After the first step is completed, the tube to measure depth is moved to the next step depth. From the tests the mean q_c/N is ranged from 4.2 to 5.6 and the total mean is 4.9. When the gained data and historical data shown in Figure 4.2 are compared, similar results are represented. It should be noticed that the standard donut-type hammer with two turning rope around the cathead was employed for the obtained data and most of the data presented in Figure 4.2. However, energy level was not corrected because the mean energy ratio in the drill rods was not gauged when the standard penetration tests were operated (Ismael & Jeragh, 1986).

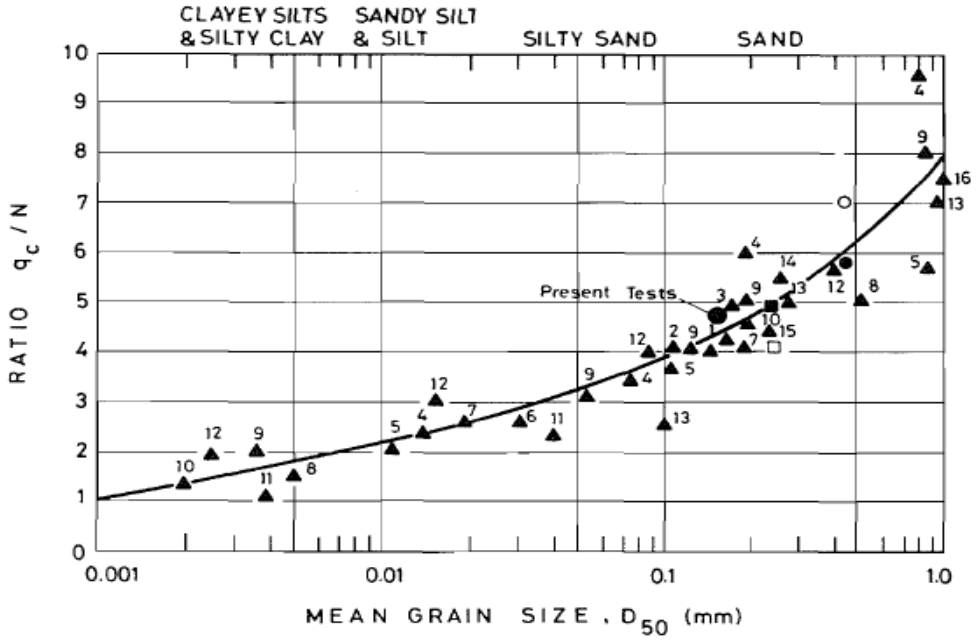

Figure 4.2 Relation between q_c/N and Mean Grain Size in Kuwait

4.2.5 Hsinta Power Plant in Taiwan

In order to arrange the initial design, 18 CPT were performed and 7 boreholes were drilled. The sites where the tests are performed have subsoil conditions divided into three strata. The peak stratum is made up of hydraulic sand fill and natural sand that have around 7m whole thickness. Under this sand stratum clay stratum is placed. Sand stratum has 35m thickness below this clay. Below 2.5 m from the ground level there is the ground water table (Chin, Duann, & Kao, 1990).

As shown by the Unified Soil Classification System (Table A-4), the peak layer that consists of the hydraulic sand fill and natural sand are normally represented as SM (sitly sand). When SPT were performed, a rope and cathead are employed to lift and fall the donut type hammer. Energy level is correlated to the 55% of the standard energy level. Cone Penetration Tests were used at overall 35 data points of sand deposits. Data from Hsinta site were put on Figure 4.3 and the data show that the bending line presented by Robertson et al. represents sensible mean, but the direct application of this bending line may lead to considerable deviation because the data shown in Figure 4.3 is on the basis of the N

value corrected by the amount of energy. If the N value had not been corrected, q_c/N would have much more spread (Chin et al., 1990).

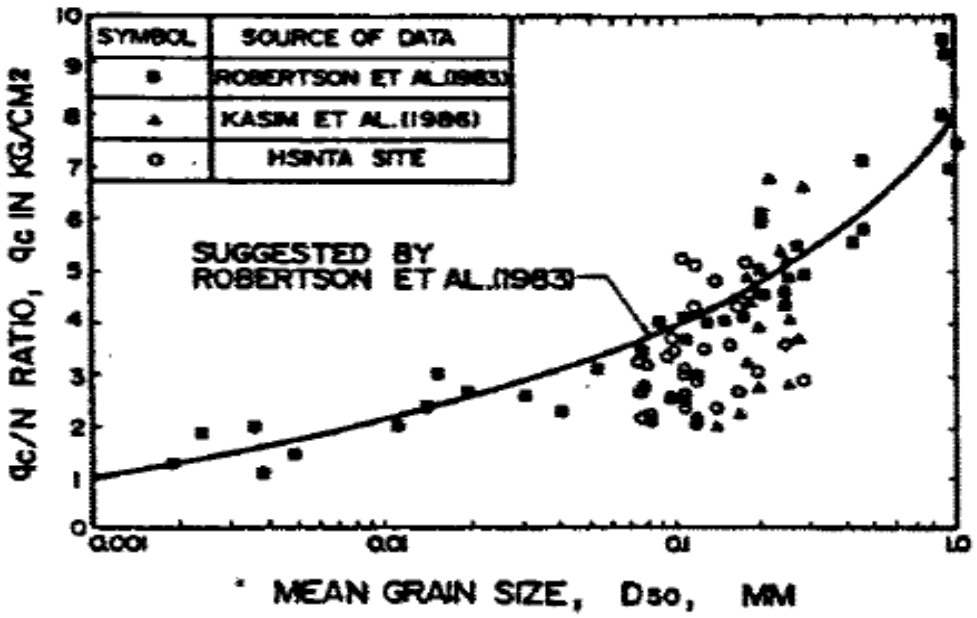

Figure 4.3 Relation between q_c/N and Mean Grain Size in Hsinta power plant and in Alameda, California

4.2.6 Harbor Bay Businees Park Project in Alameda, California

This place that has 400-acre(160-hectare) is at the end of the part in San Francisco Bay and this has smooth and level surface. In this place the correlation tests were performed and the soil is made up of hydraulic sand fill under the natural sand. The hydraulically filled sand has around 18 ft (5-1/2m) thickness. Before around 16 years, the hydraulically filled sand had been pumped into this spot. The fill can be regarded as relatively new deposits when it is compared with the Pleistocene Age natural sand which is under these new deposits(Kasim, Chu, & Jensen, 1986).

The hydraulically filled sand is represented SP-SM as shown by the Unified Soil Classification System (Table A-4). The natural sand is normally represented as SM and sometimes as SM-SC. Hogentogler type electronic cone was employed for cone penetration tests. Tip-resistance, rod inclination and side friction were measured through this cone tests. Safety

type hammer was used for SPT and during the test parameters can lead to the variation of the travelled energy and of the measured blow counts. Theses parameters were controlled to have the same energy to US standard practice and to the data shown by Robertson and Campenella(P. K. Robertson & Campanella, 1984).

Particle size analyses were carried out on 14 normal samples gained by the SPT sampler and the data about this is represented in Table A-6. Before the tests were performed, substances like clay lumps or bentonite "driller's mud" were eliminated. It is noticed that from this work and works made for other adjacent parts of the larger project sits the percentage of fines for the hydraulically filled sand and natural sand have 10% and 20%, respectively. A whole 65 test information points were chosen for the correlations in Table A-7. The relation between N and q_c was created by representing q_c as the mean over the same 12-in(30-cm) when N values were measured. The tests results from this work were represented with q_c/N and the mean grain size in Figure 4.3. The more detailed information is shown in Figure 4.4. Empty circles and triangles are used for each hydraulic and natural sands in the Figure 4.4, respectively. Although Robertson and Campanella curve indicates good average about the previous studies, the work that performed in this area are significantly spread (Kasim et al., 1986).

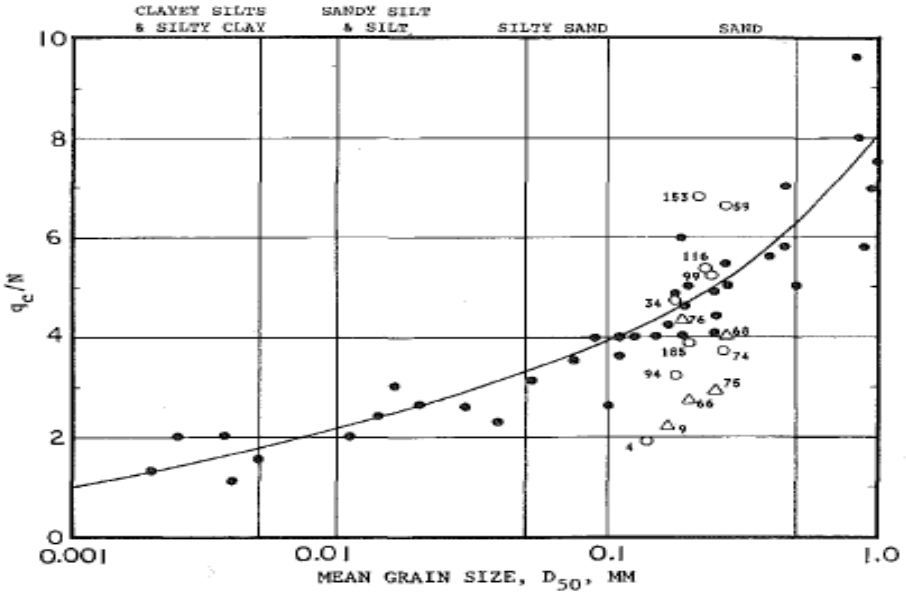

Figure 4.4 Correlation between q_c/N and mean grain size

5 Conclusion

In my conclusion and according to the studies in chapter 4, I have mentioned in the thesis, it is useful to develop the correlation between CPT and SPT, because after correlating we will obtain plentiful data based on SPT. I want to underline the importance of the correlation between the two methods, SPT and CPT.

The historical data curve of q_c/N and D_{50} were presented in the Figure 4.1 and were gained employing the standard donut-type hammer of 55% energy level and cathead system with two turns of rope. Historical data values are matched well with the values in the Tilbury island, UBC research site and Fraser river delta area in Canada. As shown in the chapter 4, when the different hammers are used or turning rope is not two times, the values of historical data are not matched well with the values in the above mentioned 3 sites.

The obtained data in Kuwait were compared with the historical data curve in Figure 4.2. However, the value gained from the Kuwait is placed a bit over the historical data curve even though the standard donut-type hammer with two turning rope around the cathead was used. The obtained data in Hsinta power plant and Harbor bay Business Park project in Alameda in California were compared with the historical data

in Figure 4.3. The test results still are scatted even if the same hammer of 55% energy level is used.

In the first 3 places in Canada, the correlation between q_c/N and D_{50} is applied after the correction of the hammer energy level to 55% so that the results are very similar to the historical data curve in Figure 4.1. In the Kuwait the correlation value between q_c/N and D_{50} is placed a bit over the historical data curve. This may be because the mean energy ratio was not recorded when the SPT was performed even though the standard donut-type hammer with two turning rope around the cathead was used. Therefore, we do not know the energy level applied in this area and that may be the reason why the historical data values and a newly gained value are a bit different. In addition, the sand in Kuwait is calcareous so that it could be the other reason (Ahmed, Agaiby, & Abdel-Rahman, 2013).

The obtained data in Hsinta power plant and Harbor bay Business Park project in Alameda in California was good. However, the data is still spread, even if the standard donut-type hammer of 55% energy and cathead system with two turns of rope were used, and soil type is not unique. Therefore, other factors could be doubted. Other information of the sites is shown in the Table A-5, Table A-6 and Table A-7. It is normally estimated that the fines content have a tendency to be inversely proportional to the q_c/N values in the data. Therefore, fines content could be the reason why the data are spread. Even though the correlation between q_c/N and D_{50} are not totally matched with the historical data, it is acceptable results to be used. Nevertheless, care has to be given when this correlation is utilized since it still needs further improvement to increase the reliability.

6 Recommendation for Further Work

From the above mentioned conclusions, it is recommended to study the correlation between q_c/N and fines content to improve the reliability of the correlation between q_c/N and D_{50} because q_c/N values are correlated with the fine content. (Chin et al., 1990). It is also recommended to study more samples about the correlation between q_c/N and D_{50} in various sites to sharpen the reliability of the q_c/N and D_{50}. When the correlation between q_c/N and D_{50} has high reliability, SPT-based data is applied for CPT. Moreover, we can save money and gain soil parameters easily by using the correlation between q_c/N and D_{50}. N-value can be estimated by using the correlation between q_c/N and D_{50} when the CPT data is obtained. The obtained N-value from the correlation has a tendency to be more correct than that from the SPT due to the repeatability problem of the SPT (Jefferies, 1993).

We can obtain other parameters such as cone sleeve friction (f_s) and friction ratio (F_r) from the CPT so that it is needed to study between N value and cone sleeve friction or friction ratio to obtain more information about the correlation between SPT and CPT (J. H. Schmertmann, 1970). In addition, each SPT and CPT results is used to obtain the potential of liquefaction so that it may be useful to study the correlation between the q_c/N and probability of liquefaction. When a site has low

probability of liquefaction, how the value of q_c/N is and when a site has high probability of liquefaction, how the value of q_c/N is.

References

Aboumatar, G. G. G. H. (1994). *Dynamic Measurements on Penetrometers for Determination of Founfdation Design.* University of Colorado.

Ahmed, S. M., Agaiby, S. W., & Abdel-Rahman, A. H. (2013). A unified CPT–SPT correlation for non-crushable and crushable cohesionless soils. *Ain Shams Engineering Journal*.

Amini, A., Fellenius, B., Sabbagh, M., Naesgaard, E., & Buehler, M. (2008). *Pile loading tests at Golden Ears Bridge.* Paper presented at the 61st Canadian Geotechnical Conference, Edmonton.

ASTM. (1984). D 1586-84 Standard Test Method for Penetration Test and Split-Barrel Sampling of Soils. *American Society for Testing and Materials*.

Baldi, G., Bellotti, R., Ghionna, V., Jamiolkowski, M., & Lo Presti, D. (1991). *Modulus of sands from CPTs and DMTs.* Paper presented at the Proc. XII ICSMFE, Rio de Janeiro.

Begemann, H. P. (1965). The friction jacket cone as an aid in determining the soil profile: JOURNAL ARTICLE-UNIDENTIFIED SOURCE.

Bieganousky, W., & Marcuson, W. (1976). Ill, 1976." Liquefaction Potential of Dams and Foundations, Report 1: Laboratory Standard Penetration Tests on Reid-Bedford Model and Ottawa Sands,". *US Army Engineer Waterways Experiment Station, CE, Vicksburg, MS, Research Report S-76-2*.

Bolton Seed, H., Tokimatsu, K., Harder, L., & Chung, R. M. (1985). Influence of SPT procedures in soil liquefaction resistance evaluations. *Journal of Geotechnical Engineering, 111*(12), 1425-1445.

Butler, F. (1974). *Heavily over-consolidated clays.* Paper presented at the Proc. Conf. Settlement of Structures, Cambridge.

C.R.I. Clayton, M. C. M. a. N. E. S. (1995). *Site investigation* (2nd ed.).

Campanella, R. (1994). *Field methods for dynamic geotechnical testing: overview of capabilities and needs.* Paper presented at the International

Symposium on Dynamic Geotechnical Testing II, 1994, San Francisco, California, USA.

Chin, C.-T., Duann, S., & Kao, T. (1990). *SPT-CPT correlations for granular soils.* Paper presented at the International Journal of Rock Mechanics and Mining Sciences and Geomechanics Abstracts.

Clayton, C. (1990). SPT energy transmission: theory, measurement and significance. *Ground Engineering, 23*(10), 33-42.

Clayton, C. R. (1995). *The standard penetration test (SPT): methods and use*: Construction Industry Research and Information Association.

Davidson, J. L., Maultsby, J. P., & Spoor, K. B. (1999). Standard penetration test energy calibrations.

De Mello, V. F. (1971). *The standard penetration test.* Paper presented at the PANAMERICAN CONGRESS ON SOIL MECHANICS AND FOUNDATION ENGINEERING.

Decourt, L. (1982). *Prediction of the bearing capacity of piles based exclusively on N values of the SPT.* Paper presented at the 2nd European Symposium of Penetration Testing, Amsterdan.

Douglas, B. J. (1982). SPT blowcount variability correlated to the CPT. *Proc. 2nd Eur. Symp.Penetration Testing, Amsterdam.*

Eslami, A. (1996). *Bearing capacity of piles from cone penetrometer test data.* Ph. D. Thesis, University of Ottawa, Department of Civil Engineering.

Eslami, A. (2006). *Bearing Capacity of Shallow and Deep Foundations from CPT Resistance.* Paper presented at the Proceedings, GeoCongress (Atlanta, Ga.), American Society of Civil Engineers, Reston, Va.

Eslami, A., & Fellenius, B. (1995). *Toe bearing capacity of piles from cone penetration test (CPT) data.* Paper presented at the Proceedings of the International Symposium on Cone Penetration Testing, CPT.

Eslami, A., & Fellenius, B. (1996). *Pile shaft capacity determined by piezocone (CPTu) data.* Paper presented at the Proceedings of 49th Canadian Geotechnical Conference, September.

Eslami, A., & Fellenius, B. H. (1997). Pile capacity by direct CPT and CPTu methods applied to 102 case histories. *Canadian Geotechnical Journal, 34*(6), 886-904.

Fairhurst, C. (1961). Wave mechanics of percussive drilling. *Mine Quarry Engng, 27*(170), 126-127.

Fellenius, B., & Eslami, A. (2000). *Soil profile interpreted from CPTu data.* Paper presented at the Proceedings of Year 2000 Geotechnics Conference, Southeast Asian Geotechnical Society, Asian Institute of Technology, Bangkok, Thailand.

Fellenius, B. H. (2014). *Basics of Foundation Design*.

Findlay, J. D. (1984). *Discussion, piling and ground treatment.* Paper presented at the Instn. Civ. Engrs. Thomas Telford, London.

Fletcher, M., & Mizon, D. (1983). *Piles in chalk for Orwell Bridge.* Paper presented at the Proc. Conf. Ground Treatment for Foundations.

Frank, R., & Magnan, J. (1996). *Cone penetration testing in France: National report.* Paper presented at the Proceedings International Symposium on Cone Penetration Testing (CPT'95).

GIBBS, H. J. a. H., W.G. (1957). *Research on determining the density of sands by spoon penetration testing.* Paper presented at the In proceedings of the 4th International Conference on Soil Mechanics, London.

Gorman, C., Drnevich, V., & Hopkins, T. (1975). Measurement of in-situ shear strength. *Situ Measurement of Soil Properties, 2*, 139-140.

Hauge, K. (1979). *Evaluation of dynamic measurement system on the standard penetration test.* University of Colorado at Boulder.

Hobbs, N. (1977). *Behaviour and design of piles in chalk-an introduction to the discussion of the papers on chalk.* Paper presented at the Proceedings, Symposium on Piles in Weak Rock.

HOLTZ.R.D (2005). [personal communication].

Horn, H. (2000). personal communication, consulting engineer, 25 Summit Road. *Verona, NJ, 7044*.

Idriss, I. (1990). *Response of soft soil sites during earthquakes.* Paper presented at the Proc. H. Bolton Seed Memorial Symposium.

Ismael, N. F., & Jeragh, A. M. (1986). Static cone tests and settlement of calcareous desert sands. *Canadian Geotechnical Journal, 23*(3), 297-303.

IWASAKI, Y. O. a. R. (1973). On dynamic shear moduli and Poisson's ratios of soil deposits. *The Japanese Geotechnical Society*.

Jamiolkowski, M., Lo Presti, D., & Manassero, M. (2001). *Evaluation of relative density and shear strength of sands from CPT and DMT.* Paper presented at the Soil behavior and soft ground construction.

Jefferies, M. G. a. D., M.P. (1993). Estimation of SPT N values from the CPT. *ASTM*.

Juang, C. H., Chen, C. J., Jiang, T., & Andrus, R. D. (2000). Risk-based liquefaction potential evaluation using standard penetration tests. *Canadian Geotechnical Journal, 37*(6), 1195-1208.

Kanai, K., Tanaka, T., Morishita, T., & Osada, K. (1967). Observation of Microtremors. XI.: Matsushiro Earthquake Swarm Area.

Karl, L., Haegeman, W., & Degrande, G. (2006). Determination of the material damping ratio and the shear wave velocity with the seismic cone penetration test. *Soil dynamics and earthquake engineering, 26*(12), 1111-1126.

Kasim, A. G., Chu, M.-Y., & Jensen, C. N. (1986). Field correlation of cone and standard penetration tests. *Journal of Geotechnical Engineering, 112*(3), 368-372.

Kovacs, W., Griffith, A., & Evans, J. (1978). An Alternative to the Cathead and Rope for the Standard Penetration Test. *ASTM Geotechnical Testing Journal, 1*(2).

Kovacs, W., Yokel, F., Salomone, L., & Holtz, R. (1984). *Liquefaction potential and the international SPT.* Paper presented at the Proceedings of the Eighth World Conference on Earthquake Engineering.

Kovacs, W. D., & Salomone, L. A. (1982). SPT hammer energy measurement. *J. Geotech. Eng. Div., Am. Soc. Civ. Eng.;(United States), 108*.

Kulhawy, F. H., & Mayne, P. W. (1990). Manual on estimating soil properties for foundation design: Electric Power Research Inst., Palo Alto, CA (USA); Cornell Univ., Ithaca, NY (USA). Geotechnical Engineering Group.

Ladd, C. (1977). Stress-deformation and strength characteristics, state of the art report. *Proc. of 9th ISFMFE., 1977, 4*, 421-494.

Liao, S. S., & Whitman, R. V. (1986). Overburden correction factors for SPT in sand. *Journal of Geotechnical Engineering, 112*(3), 373-377.

Lousberg, M., & Calembert, L. (1974). *Penetration testing in Belgium.* Paper presented at the Proceedings 1st European Symposium on Penetration Testing, ESOPT-1, Stockholm.

Lunne, T., & Keaveny, J. (1995). *Technical report on solution of practical problems using CPT.* Paper presented at the International Symposium on Cone Penetration Testing, CPT.

Lunne, T., Robertson, P., & Powell, J. (1997). Cone penetration testing. *Geotechnical Practice*.

MARCUSON, W. F., iii , BALLARD,R.F.,JR., and COOPER,S.S. (1978). *Comparison of penetration resistance values to in situ shear wave velocities.* Paper presented at the Proceedings of the Second International Conference on Microzonation for Safer Construction-Research and Application, San Francisco.

Martin, R. E., Seli, J. J., Powell, G. W., & Bertoulin, M. (1987). Concrete pile design in Tidewater Virginia. *Journal of Geotechnical Engineering, 113*(6), 568-585.

Martins, J. B., and Furtado,R. (1963). *Standard penetration test and deep sounding test foundation engineering*. Paper presented at the Africa soil mechanics and foundations engineering,Salisbury,Zimbabwe.

Mayne, P. (2007). NCHRP Synthesis 368—Cone Penetration Testing. *Transportation Research Board, Washington, DC*.

Mayne, P. W., & Rix, G. J. (1995). Correlations between shear wave velocity and cone tip resistance in natural clays. *Soils and Foundations, 35*(2), 107-110.

Meigh, A. (1987). *Cone penetration testing: methods and interpretation*.

Meisina, D. L. P. a. C. (2013). *CPT HANDBOOK "Use of cone penetration tests for soil profiling and design of shallow and deep foundations".* PAGANI GEOTECHNICAL EQUIPMENT.

Meyerhof, G. (1956). Penetration tests and bearing capacity of cohesionless soils. *Journal of the Soil Mechanics and Foundation Division, 82*(1), 1-19.

Mitchell, J. K., & Gardner, W. S. (1975). *In situ measurement of volume change characteristics.* Paper presented at the In Situ Measurement of Soil Properties.

Navy, U. (1986). Soil Mechanics Design Manual 7.1, NAVFAC DM-7.1: Department of the Navy, Naval Facilities Engineering Command, Alexandria, VA.

Olsen, R. S. (1997). Cyclic liquefaction based on the cone penetrometer test *Technical Report NCEER* (Vol. 97, pp. 225-276): US National Center for Earthquake Engineering Research (NCEER).

Poulos, H. G. (1989). Pile behaviour—theory and application. *Geotechnique, 39*(3), 365-415.

Rauch, A. (1998). Personal Communication.(as cited in Youd, TL 2001- "Liquefaction Resistance of Soils: Summary Report from the 1996 NCEER and 1998 NCEER/NSF Workshops on Evaluation of Liquefaction Resistance of Soils". *Journal of Geotechnical and Geo environmental Engineering, ASCE*.

Robertson, P. (1990). Soil classification using the cone penetration test. *Canadian Geotechnical Journal, 27*(1), 151-158.

Robertson, P. (2010a). Evaluation of flow liquefaction and liquefied strength using the cone penetration test. *Journal of Geotechnical and Geoenvironmental Engineering, 136*(6), 842-853.

Robertson, P. (2010b). *Soil behaviour type from the CPT: an update.* Paper presented at the 2nd International Symposium on Cone Penetration Testing, USA.

Robertson, P., Campanella, R., & Wightman, A. (1983). Spt-Cpt Correlations. *Journal of Geotechnical Engineering, 109*(11), 1449-1459.

Robertson, P., & Wride, C. (1998). Evaluating cyclic liquefaction potential using the cone penetration test. *Canadian Geotechnical Journal, 35*(3), 442-459.

Robertson, P. K. (1986). In situ testing and its application to foundation engineering. *Canadian Geotechnical Journal, 23*(4), 573-594.

Robertson, P. K., & Campanella, R. (1983). Interpretation of cone penetration tests. Part I: Sand. *Canadian Geotechnical Journal, 20*(4), 718-733.

Robertson, P. K., & Campanella, R. (1984). *Guidelines for use and interpretation of the electronic cone penetration test*: University of British Columbia, Department of Civil Engineering.

Robertson, P. K., Campanella, R., Gillespie, D., & Greig, J. (1986). *Use of piezometer cone data.* Paper presented at the Use of in situ tests in geotechnical engineering.

Robertson, P. K., Fear, C., Youd, T. L., & Idriss, I. M. (1997). Cyclic liquefaction and its evaluation based on the SPT and CPT. *Technical Report NCEER, 97*, 41-87.

Robertson, P. K., Woeller, D. J., & Addo, K. O. (1992). Standard penetration test energy measurements using a system based on the personal computer. *Canadian Geotechnical Journal, 29*(4), 551-557.

Rogers, J. D. (2006). Subsurface exploration using the standard penetration test and the cone penetrometer test. *Environmental & Engineering Geoscience, 12*(2), 161-179.

Sanglerat, G. (1972). The Penetrometer and Soil Exploration (pp. 488): Elsevier Publishing Company, Amsterdam, The Netherlands.

Schmertmann, J. (1976). Predicting the q c/N Ratio. *Engineering and Industrial Experiment Station. Department of Civil Engineering, University of Florida, Gainesville, Final Report D-636*.

Schmertmann, J., Smith, T., & Ho, R. (1978). EXAMPLE OF AN ENERGY CALIBRATION REPORT ON A PENETRATION TEST (ASTM STANDARD D 1586-67) DRILL RIG. *ASTM Geotechnical Testing Journal, 1*(1).

Schmertmann, J. H. (1970). Static cone to compute static settlement over sand. *Journal of Soil Mechanics & Foundations Div*.

Schmertmann, J. H. (1978). GUIDELINES FOR CONE PENETRATION TEST.(PERFORMANCE AND DESIGN).

Schmertmann, J. H., & Palacios, A. (1979). Energy dynamics of SPT. *Journal of the Geotechnical Engineering Division, 105*(8), 909-926.

Schnaid, F. (2005). *Geocharacterisation and properties of natural soils by in situ tests.* Paper presented at the PROCEEDINGS OF THE INTERNATIONAL CONFERENCE ON SOIL MECHANICS AND GEOTECHNICAL ENGINEERING.

Schnaid, F. (2009). *In situ testing in geomechanics: the main tests*: CRC Press.

Shioi, Y., & Fukui, J. (1982). *Application of N-value to design of foundations in Japan.* Paper presented at the Proceeding of the Second European Symposium on Penetration Testing.

Skempton, A. (1986). Standard penetration test procedures and the effects in sands of overburden pressure, relative density, particle size, ageing and overconsolidation. *Geotechnique, 36*(3), 425-447.

Sowers, G. F. (1979). *Introductory Soil Mechanics and Foundations, 4th edition*. Macmillan,New York.

Stark, T. D., & Olson, S. M. (1995). Liquefaction resistance using CPT and field case histories. *Journal of Geotechnical Engineering, 121*(12), 856-869.

Stroud, M. (1974). *The standard penetration test in insensitive clays and soft rocks.* Paper presented at the Proc. European Symposium on Penetration Testing, Stockholm.

Suzuki, Y., Tokimatsu, K., Koyamada, K., Taya, Y., & Kubota, Y. (1995). *Field correlation of soil liquefaction based on CPT data.* Paper presented at the Proceedings, International Symposium on Cone Penetration Testing, CPT.

Tand, K. E., Funegard, E. G., & Briaud, J.-L. (1986). *Bearing Capacity of Footings on Clay CPT Method.* Paper presented at the Use of In Situ Tests in Geotechnical Engineering.

Thorburn, S., & Mac Vicar, R. (1971). *Pile load tests to failure in the Clyde alluvium.* Paper presented at the Proceedings of the Conference on Behaviour of Piles.

Wright, S., & Reese, L. (1979). Design of large diameter bored piles. *Ground Engineering, 12*(8), 17-51.

Yamashita, K., Tomono, M., & Kakurai, M. (1987). A method for estimating immediate settlement of piles and pile groups. *Soils and Foundations, 27*(1), 61-76.

Youd, T., & Idris, I. (1997). Summary Report: Proceedings of the NCEER Workshop On Evaluation of Liquefaction Resistance of Soils: NCEER.

Youd, T., Idriss, I., Andrus, R. D., Arango, I., Castro, G., Christian, J. T., . . . Hynes, M. E. (2001). Liquefaction resistance of soils: summary report from the 1996 NCEER and 1998 NCEER/NSF workshops on evaluation of liquefaction resistance of soils. *Journal of Geotechnical and Geoenvironmental Engineering, 127*(10), 817-833.

Zhang. (2009). Standard Penetration Test.

Appendix A

Table A-1 Types of Sampler

Sampler	Disturbed/ Undisturbed	Appropriate Soil Types	Method of Penetration	% Use in Practice
Split-Barrel (Split Spoon)	Disturbed	Sands, silts, clays	Hammer driven	85
Thin-Walled Shelby Tube	Undisturbed	Clays, silts, fine-grained soils, clayey sands	Mechanically Pushed	6
Continuous Push	Partially Undisturbed	Sands, silts,& clays	Hydraulic push with plastic lining	4
Piston	Undisturbed	Silts and clays	Hydraulic Push	1
Pitcher	Undisturbed	Stiff to hard clay, silt, sand, partially weather rock, and frozen or resin impregnated granular soil	Rotation and hydraulic pressure	< 1
Denison	Undisturbed	Stiff to hard clay, silt, sand and partially weather rock	Rotation and hydraulic pressure	< 1
Modified California	Disturbed	Sands, silts, clays, and gravels	Hammer driven (large split spoon)	< 1

Continuous Auger	Disturbed	Cohesive soils	Drilling with Hollow Stem Augers	< 1
Bulk	Disturbed	Gravels, Sands, Silts, Clays	Hand tools, bucket augering	< 1
Block	Undisturbed	Cohesive soils and frozen or resin impregnated granular soil	Hand tools	< 1

Table A-2 Energy Ratio in the Countries Depending on the Hammer and Release Types (Skempton, 1986)

Country	Hammer	Release	ER_r (%)	$ER_r/60$
Japan	Donut	Tombi	78	1.3
	Donut	2 turns of rope	65	1.1
China	Pilcon type	Trip	60	1.0
	Donut	Manual	55	0.9
USA	Safety	2 turns of rope	55	0.9
	Donut	2 turns of rope	45	0.75
UK	Pilcon, Dando,	Trip	60	1.0
	Old standard	2 turns of rope	50	0.8

Table A-3 Grain Size Scale

Size range (metric)	Aggregate name (Wentworth Class)
>256 mm	Boulder
64–256 mm	Cobble
32–64 mm	Very coarse gravel
16–32 mm	Coarse gravel
8–16 mm	Medium gravel
4–8 mm	Fine gravel
2–4 mm	Very fine gravel
1–2 mm	Very coarse sand
0.5–1 mm	Coarse sand
0.25–5mm	Medium sand
0.125–0.250 mm	Fine sand
0.0625–0.125 mm	Very fine sand
0.00390625–0.0625 mm	Silt
< 0.00390625 mm	Clay
< 0.001 mm	Colloid

Table A-4 Unified Soil Classification System

Major divisions	Group symbol	Group name

Coarse grained soils more than 50% retained on or above No.200 (0.075mm)sieve	gravel>50% of coarse fraction retained on No.4(4.75mm)sieve	clean gravel < 5% smaller than #200 Sieve	GW	well-graded gravel, fine to coarse gravel
			GP	Poorly graded gravel
		Gravel with¿12% fines	GM	silty gravel
			GC	clayey gravel
	sand≥ 50% of coarse fraction passes No.4 sieve	clean sand	SW	well-graded sand, fine to coarse sand
			SP	poorly graded sand
		Sand with >12% fines	SM	silty sand
			SC	clayey sand
Fine grained soils 50% or more passing the No.200 sieve	silt and clay liquid limit < 50	inorganic	ML	silt
			CL	clay of low plasticity, lean clay
		organic	OL	organic silt, organic clay
	silt and clay liquid limit ≥50	Inorganic	MH	silt of high plasticity, elastic silt
			CH	clay of high plasticity, fat clay
		organic	OH	organic clay, organic silt

Highly organic soils	Pt	Peat

Table A-5 Data of SPT, CPT and Particle Size in Hsinta Site

Depth (m)	N_{55}	q_c (kg/cm^2)	Friction Ratio (%)	Fine Content (%)	D_{50} (mm)
2.0	12.85	48.14	0.26	35	0.1
4.0	5.00	13.46	0.43	25	0.17
38.5	39.96	134.84	0.78	25	0.095
44.5	77.07	170.65	1.27	44	0.083
21.0	30.68	106.59	0.91	23	0.100
31.0	29.29	62.32	0.30	37	0.084
33.0	19.52	63.65	0.28	46	0.078
37.0	23.71	76.19	0.40	45	0.081
1.0	14.97	64.87	0.73	28	0.120
2.0	11.23	49.06	0.49	25	0.170
3.0	8.73	42.02	0.48	18	0.140
4.0	14.97	46.21	0.56	21	0.200
21.0	41.16	99.45	0.82	18	0.110
31.0	24.95	73.24	0.45	37	0.120
37.0	47.40	131.07	1.03	46	0.080
39.0	51.14	153.51	1.25	34	0.120
41.0	52.39	184.93	1.82	33	0.130
5.0	16.73	48.55	0.04	13	0.290

37.0	51.19	114.04	0.63	24	0.170
5.0	11.75	54.16	0.02	17	0.180
20.5	41.17	88.03	0.81	18	0.120
28.5	26.11	94.55	0.10	24	0.250
34.5	45.69	108.43	0.29	25	0.140
36.5	18.28	93.53	0.54	34	0.120
40.5	56.13	150.25	0.89	48	0.077
42.5	67.88	169.93	1.45	32	0.110
48.5	48.30	104.86	1.17	46	0.080
2.0	8.56	44.68	0.41	17	0.110
3.0	7.14	36.92	0.29	15	0.180
5.0	17.12	61.71	0.29	23	0.260
21.5	27.12	70.99	0.93	36	0.110
33.5	29.97	61.40	0.36	31	0.120
37.5	41.39	129.44	1.22	28	0.110
39.5	68.51	208.08	1.22	21	0.110
45.5	67.01	183.80	1.78	47	0.080

Table A-6 Particle Size Data in Alameda, California

Sample # (1)	D50(mm) (2)	Fines (%) (3)	Passing Sieve (%)		
			#30 (4)	#50 (5)	#100 (6)
1	0.2	9	99	84	25
2	0.18	11	100	94	31

3	0.14	19	100	99	52
4	0.17	31	100	99	38
5	0.25	3	99	71	11
6	0.2	17	99	76	28
7	0.28	5	98	58	9
8	0.18	7	100	94	28
9	0.27	6	99	57	8
10	0.22	6	100	79	15
11	0.18	26	100	81	41
12	0.24	18	99	63	25
13	0.25	15	99	60	21
14	0.26	20	100	56	25

Table A-7 Penetration records in Alameda, California

Depth (ft) (1)	Measured N^b (2)	Corrected N (3)	q_c (kg/cm^2) (4)	Depth (ft) (5)	Measured N^b (6)	Corrected N (7)	q_c (kg/cm^2) (8)
(a) Test Location 1				(e) Test Location 5			
2	25	25	106	3	19	19	115
5	27	27	123	6(7)	9	9	59
8	28	28	119	35.2*	49	49	80
14.6	26	26	113	(f) Test Location 6			
17.1	6	6	41	3	31(1)	41.3	236
34.2*	10	10	60	6	26(1)	34.7	142

37.2*	53	53	184	9(8)	22(1)	29.3	94
(b) Test Location 2				33.7*	41(1)	54.7	180
2	29	29	156	(g) Test Location 7			
5	62	62	271	3	34(1)	45.3	254
8	31	31	186	6	39(1)	52	285
11.1	18	18	103	9	40(1)	53.3	293
14.1	21	21	79	12.1	47(1)	62.7	242
17.1	8	8	50	18.1(9)	15(1)	20	74
28.6*	9	9	30	21.1*	5(1)	6.7	33
31.2*	24	24	54	24.1*	18(1)	24	171
34.2*	31	31	110	(h) Test Location 8			
(C) Test Location 3				2.5(10)	17(1)	22.7	153
3	39	39	152	5.5	33(1)	44	230
6(1)	47	47	185	8.5	43(1)	57.3	231
9	36	36	133	11.6	54	54	350
12	19	19	76	17.6	12(1)	16	42
15.1(2)	7	7	34	20.6*	5(1)	6.7	17
18.1(3)	2	2	4	23.6*(11)	13(1)	17.3	76

33.2*(4)	4	4	9	26.6*	9(1)	12	241
37.2*	27	27	67	(i) Test Location 9			
(d) Test Location 4				6.1	21(2)	35	119
3	12	12	80	7.6	32(2)	53.3	85
6	28	28	155	9.1	19(2)	31.7	79
9	25	25	157	10.7	6(2)	10	63
12(5)	19	19	99	15.2	23(2)	38.3	180
15.1	30	30	145	17.2(12)	13(2)	21.7	116
29.2*(6)	24	24	66	19.2*	11(2)	18.3	67
34.2*	40	40	133	20.7*(13)	16(2)	26.7	75
39.2*	32	32	196	23.2*	28(2)	46.7	172
				31.3*	25(2)	41.7	107
				40.2(14)	10(2)	16.7	68

Note: [a]Depth represents the half point of SPT. *marks beside the depth indicate natural sand and other one indicates hydraulically filled sand. Numbers in parentheses beside the depth indicate the sampler numbers in Table A-5.

[b]SPT procedures: SPT performed with safety hammer and three times binding, and N is related to the standard energy ratio 55%. (1) SPT was carried out with safety hammer and two times binding but it was corrected to the standard donut hammer and two times binding as shown by Kocacs (W. D. Kovacs & Salomone, 1982) (W. Kovacs, Yokel, Salomone, & Holtz, 1984) or (2) SPT was performed employing no liners for sampler to be employed with liner, and safety hammer and two times binding was employed. However, it was corrected as above (1).

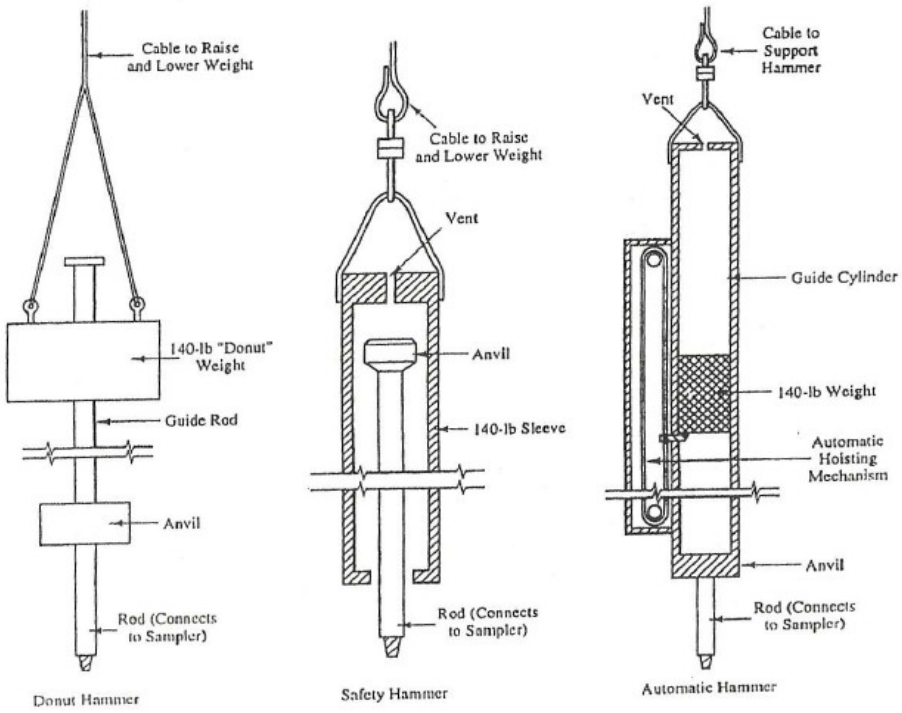

Figure A-1 Types of Hammers

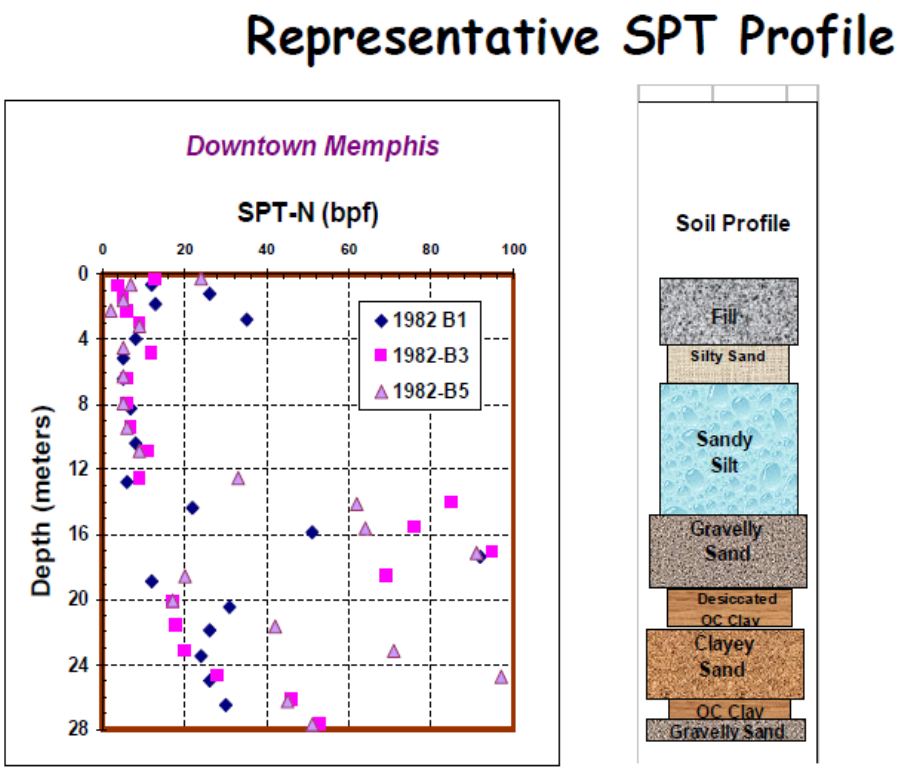

Figure A-2 Example of soil classification by SPT